Different complex regulatory phenotypes underlie hybrid male sterility in divergent rodent crosses

Kelsie E. Hunnicutt[*,1], Colin Callahan[2], Sara Keeble[2], Emily C. Moore[1,2], Jeffrey M. Good[2], and Erica L. Larson[*,1]

[1] University of Denver, Department of Biological Sciences, Denver, CO, 80208
[2] Division of Biological Sciences, University of Montana, Missoula, MT, 59812
*Corresponding authors

ORCID: 0000-0002-9674-0630 (KEH)
ORCID: 0000-0002-0385-1121 (CC)
ORCID: 0000-0002-7318-3122 (SK)
ORCID: 0000-0001-6166-3367 (ECM)
ORCID: 0000-0003-0707-5374 (JMG)
ORCID: 0000-0003-3006-645X (ELL)

Corresponding Authors:
Kelsie Hunnicutt
Department of Biological Sciences
University of Denver
Denver, CO 80208
Email: Kelsie.Hunnicutt@du.edu

Erica Larson
Department of Biological Sciences
University of Denver
Denver, CO 80208
Email: Erica.Larson@du.edu

Running title: Rodent hybrid male sterility

Key words: speciation, hybrid male sterility, gene expression, fluorescence activated cell sorting, meiotic sex chromosome inactivation, *Phodopus*

ABSTRACT

Hybrid incompatibilities are a critical component of species barriers and may arise due to negative interactions between divergent regulatory elements in parental species. We used a comparative approach to identify common themes in the regulatory phenotypes associated with hybrid male sterility in two divergent rodent crosses, dwarf hamsters and house mice. We investigated three potential characteristic gene expression phenotypes in hybrids including the propensity of transgressive differentially expressed genes in hybrids towards over or underexpression relative to parental species, the influence of developmental stage on the extent of misexpression, and the role of the sex chromosomes on misexpression phenotypes. In contrast to near pervasive overexpression in hybrid house mice, we found that misexpression in hybrid dwarf hamsters was dependent on developmental stage. In both house mouse and dwarf hamster hybrids, however, transgressive misexpression increased with the progression of spermatogenesis, although to varying extents and with potentially different consequences. In both systems, we detected sex-chromosome specific overexpression in stages of spermatogenesis where inactivated X chromosome expression was expected, but the hybrid overexpression phenotypes were fundamentally different. Importantly, misexpression phenotypes support the presence of multiple developmental blocks to spermatogenesis in dwarf hamster hybrids, including a potential role of meiotic stalling or breakdown early in spermatogenesis. Collectively, we demonstrate that while there are some similarities in hybrid expression phenotypes of house mice and dwarf hamsters, there are also clear differences that point towards unique mechanisms underlying hybrid male sterility in each system. Our results highlight the potential of comparative approaches in helping to understand the causes and consequences of disrupted gene expression in speciation.

INTRODUCTION

The evolution of postzygotic reproductive barriers, such as hybrid inviability and sterility, is an important part of the speciation process, and identifying the genetic architecture of hybrid incompatibilities has been a common goal uniting speciation research (Coughlan and Matute 2020). While identifying the genetic basis of hybrid dysfunction remains difficult in many systems, downstream regulatory phenotypes can provide insight into the underlying mechanisms of speciation (Mack and Nachman 2017). An outstanding question surrounding the role of disrupted gene regulation and speciation is whether the combination of two divergent genomes in hybrids results in gene expression perturbations that are consistent or repeatable across species. At the broadest level, it is unclear whether gene expression in hybrids tends to be intermediate or transgressive (outside the range of parental gene expression), whether transgressive gene expression is biased towards over or underexpression (Ortíz-Barrientos *et al.* 2007), and whether misexpression tends to be modulated by *cis* or *trans* regulatory elements (Wittkopp *et al.* 2004; McManus *et al.* 2010; Oka *et al.* 2014; Mack *et al.* 2016; Mugal *et al.* 2020; Kopania *et al.* 2022a). By investigating trends in the magnitude and direction of transgressive expression across different hybrid systems, we can begin to understand the evolutionary forces shaping regulatory-based hybrid incompatibilities. For example, if expression in hybrids tends towards overexpression, this may mean that genes contributing to hybrid incompatibilities are normally repressed in parental lineages (Meiklejohn *et al.* 2014; Barreto *et al.* 2015; Larson *et al.* 2017). Alternatively, expression in hybrids may tend towards underexpression if regulatory divergence between parental lineages results in impaired transcription factor binding with promoter or enhancer elements (Oka *et al.* 2014; Guerrero *et al.* 2016) or if divergence stimulates epigenetic silencing (Paun *et al.* 2007; Shivaprasad *et al.* 2012; Lafon-Placette and Köhler 2015; Brekke *et al.* 2016; Zhu *et al.* 2017).

At a finer scale, misexpression patterns may depend on developmental stage: for example, if there is greater pleiotropy earlier in development (Ortíz-Barrientos *et al.* 2007; Cutter and Bundus 2020). In particular, we might expect sterile hybrids to have more misexpression during later stages of gametogenesis when genes are evolving rapidly and are potentially under less regulatory constraint (Kopania *et al.* 2022a; Murat *et al.* 2023). Finally, the role of sex chromosome regulation in inviable or sterile hybrids encompasses both of these larger questions. Sex chromosomes may be prone to asymmetry in their expression divergence (Oka and Shiroishi 2014; Civetta 2016) and be regulated differently across stages of development (Presgraves 2008; Larson *et al.* 2018), particularly in reproductive tissues, and thus may play a central role in hybrid dysregulation relative to autosomes.

Disruption of sex chromosome regulation is thought to be a potentially widespread regulatory phenotype in sterile hybrids (Lifschytz and Lindsley 1972; Larson *et al.* 2018), in part because X chromosome repression may be crucial to normal spermatogenesis in diverse taxa (McKee and Handel 1993; Landeen *et al.* 2016; Taxiarchi *et al.* 2019; Rappaport *et al.* 2021; Viera *et al.* 2021; Murat *et al.* 2023). Furthermore, misregulation of the X chromosome is associated with hybrid sterility in several species pairs (Davis *et al.* 2015; Sánchez-Ramírez *et al.* 2021; Bredemeyer *et al.* 2021), although it has been best studied in house mice. In fertile male mice, the X chromosome is silenced early in meiosis through meiotic sex chromosome inactivation (MSCI; McKee and Handel 1993; Handel 2004) and is again repressed in postmeiotic sperm development (*i.e.,* postmeiotic sex chromosome repression or PSCR; Namekawa *et al.* 2006). In contrast, the X chromosome is not properly inactivated and is overexpressed in sterile hybrid mice (Good *et al.* 2010; Bhattacharyya *et al.* 2013; Campbell *et al.* 2013; Turner *et al.* 2014; Larson *et al.* 2017, 2022). Disrupted MSCI in house mice is associated with divergence at *Prdm9*, a gene that is a major contributor to hybrid male sterility (Mihola *et al.* 2009; Davies *et al.* 2016). However, misexpression of the X chromosome in sterile

75 hybrids could result from mechanisms other than *Prdm9*-associated disrupted MSCI, such as
76 mispairing of the sex chromosomes due to divergence in their region of homology known as
77 the pseudoautosomal region (PAR; Burgoyne 1982; Ellis and Goodfellow 1989; Raudsepp and
78 Chowdhary 2015). In sum, the ubiquity of X chromosome repression and the growing body of
79 evidence linking disrupted MSCI to hybrid sterility in mammals suggest that disrupted sex
80 chromosome regulation may be a common regulatory phenotype in sterile hybrid males.
81 Here, we characterized disruption of gene expression associated with hybrid male
82 sterility in two rodent crosses, dwarf hamsters and house mice, which span ~35 million years
83 of divergence (Swanson *et al.* 2019). The regulatory phenotypes of hybrid male sterility have
84 been thoroughly studied in house mice (Good *et al.* 2010; Bhattacharyya *et al.* 2013; Campbell
85 *et al.* 2013; Turner *et al.* 2014; Larson *et al.* 2017, 2022; Hunnicutt *et al.* 2022). We contrast
86 these with an analogous cross between two sister species of dwarf hamster, Campbell's dwarf
87 hamster (*Phodopus campbelli*) and the Siberian dwarf hamster (*P. sungorus*), and their sterile
88 F1 hybrid male offspring. These species diverged only ~0.8-1.0 million years ago (Neumann *et*
89 *al.* 2006), and they are not thought to interbreed in the wild due to geographic separation
90 (Ishishita *et al.* 2015). Crosses between female *P. sungorus* and male *P. campbelli* produce
91 sterile hybrid males that, similar to mice, have a range of sterility phenotypes, suggesting
92 multiple developmental blocks to spermatogenesis (Ishishita *et al.* 2015; Bikchurina *et al.*
93 2018). Hybrids from the reciprocal cross are usually inviable due to abnormal growth *in utero*
94 (Brekke and Good 2014), and the species origin of the X chromosome is the primary genetic
95 factor controlling hybrid inviability (Brekke *et al.* 2021). Additionally, sex chromosome
96 asynapsis during spermatogenesis is common in hybrid dwarf hamsters, providing further
97 reason to think that X chromosome-specific misregulation may be observed in sterile hybrid
98 dwarf hamsters (Ishishita *et al.* 2015; Bikchurina *et al.* 2018). Both the abnormal spermatogenic
99 phenotypes observed in dwarf hamster hybrids and the potential regulatory interactions that

100 may result from the involvement of the X chromosome in multiple reproductive barriers make
101 dwarf hamsters an important comparison to mice for investigating what regulatory phenotypes
102 may be repeatedly associated with the evolution of postzygotic reproductive isolation.

103 Expression phenotypes associated with hybrid sterility have historically been difficult to
104 assess because of the cellular diversity of reproductive tissues (*e.g.,* testes; Good *et al.* 2010;
105 Ramm and Schärer 2014; Montgomery and Mank 2016; Hunnicutt *et al.* 2022), thus requiring
106 molecular approaches that permit greater spatial and developmental resolution into expression
107 evolution. To overcome these difficulties, we used Fluorescence Activated Cell Sorting (FACS)
108 to isolate and sequence cell populations across the developmental timeline of
109 spermatogenesis for each species pair and their F1 hybrids, including stages that span the
110 different sex chromosome regulatory states. We used both datasets to address three main
111 questions about the gene expression phenotypes observed in sterile hybrids: (1) within
112 transgressive differentially expressed genes, does misexpression tend towards up- or
113 downregulation in hybrids compared to parents? (2) are there similar patterns of disrupted
114 expression across stages of development? and (3) are there clear differences between
115 autosomes and sex chromosomes in regulatory phenotypes? And if so, is sex chromosome-
116 specific misexpression consistent with either disrupted MSCI and/or disrupted PAR regulation?
117 Collectively, we demonstrate the power of cell type-specific approaches for untangling the
118 expression phenotypes associated with the evolution of hybrid male sterility and for identifying
119 common themes in the mechanistic basis of hybrid incompatibilities across divergent taxa.

120 MATERIALS AND METHODS

121 Hamster crosses and male reproductive phenotypes

122 We used wild-derived colonies of two sister species of dwarf hamster, *P. sungorus* and
123 *P. campbelli*, established by Kathy Wynne-Edwards (Scribner and Wynne-Edwards 1994) and

124 housed at the University of Montana. Both species were maintained as closed colonies with a
125 breeding scheme to minimize inbreeding. Nonetheless, inbreeding levels of these closed
126 colonies are still high as indicated by very low nucleotide diversity (Brekke *et al.* 2018). We
127 used males from both parent species and male F1 hybrid offspring from crosses of female *P.*
128 *campbelli* with male *P. sungorus*. We weaned males in same-sex sibling groups between 17 -
129 21 dpp and housed them individually at 45 dpp. We euthanized reproductively mature males
130 using carbon dioxide followed by cervical dislocation between 59 - 200 dpp (Table S1). All
131 animal use was approved by the University of Montana (IACUC protocols 050-16JGDBS &
132 035-19JGDBS).

133 We measured several fertility metrics for parent species and hybrid males including
134 paired testes weight, paired seminal vesicle weight, normalized sperm counts, and sperm
135 motility (Good *et al.* 2008). Paired testes weight and paired seminal vesicle weight were
136 correlated with body weight (paired testes weight Pearson's $r(29) = 0.47$, $p = 0.007$; paired
137 seminal vesicle weight Pearson's $r(23) = 0.56$, $p = 0.003$), so we standardized both metrics
138 relative to body weight. We calculated sperm count by isolating sperm from caudal
139 epididymides diced in 1 ml of Dulbecco's PBS (Sigma) and incubated at 37°C for 10 minutes.
140 We quantified sperm motility (proportion of motile sperm in a 5 µl suspension) and sperm count
141 (number of sperm with head and tail in a heat shocked 5 µl suspension) across a fixed area on
142 a Makler counting chamber. We performed statistical comparisons of fertility phenotypes in R
143 v.4.3.1, and we used the FSA package v.0.9.4 for the Kruskal-Wallis and Dunn's tests (Ogle
144 and Ogle 2017).

145

146 **Isolation of enriched cell populations from hamster testes**

147 To investigate the regulatory dynamics of the sex chromosomes during
148 spermatogenesis, we isolated four spermatogenic cell populations from whole testes using

149 FACS: spermatogonia, leptotene/zygotene spermatocytes, diplotene spermatocytes, and
150 round spermatids. Briefly, we disassociated a single testis per male following a published
151 protocol originally developed for house mice (Getun *et al.* 2011) with modifications
152 (github.com/goodest-goodlab/good-protocols/tree/main/protocols/FACS, last accessed June
153 16, 2021). We doubled the volumes of all reagents to account for the increased mass of testes
154 in dwarf hamsters relative to house mice. We isolated cell populations based on size,
155 granularity, and fluorescence on a FACSAria IIu cell sorter (BD Biosciences) at the University of
156 Montana Center for Environmental Health Sciences Fluorescence Cytometry Core. For each
157 sorted cell population, we extracted RNA using RNeasy kits (Qiagen) following protocols for
158 Purification of Total RNA from Animal Cells. We quantified sample RNA quantity and quality
159 (requiring an RNA integrity number > 7) on a Tapestation 2200 (Agilent) at the University of
160 Montana genomics core. RNA libraries were prepared by Novogene and sequenced on Illumina
161 NovaSeq 6000s (paired end, 150 bp). Six samples (distributed across different species and cell
162 types) had low RNA concentrations, and for these samples we used Novogene's low input
163 RNA library preparation (Table S2). MDS plots indicated no severe library batch effects
164 between samples from different library preparations (Figure S1), so we included all samples
165 from both libraries in subsequent analyses.
166
167 **Read processing and mapping**
168 We sequenced RNA from each cell population for three to five individuals of each
169 parent species and F1 hybrids generating an average of ~27.5 million read pairs per individual
170 (Table S2). We trimmed reads using Trimmomatic v.0.39 (Bolger *et al.* 2014) to remove low
171 quality bases from the first and last 5 bp of each read and bases with an average Phred score
172 of less than 15 across a 4 bp sliding window and only retained reads of at least 36 bp. We next
173 used an approach (based on the modtools pipeline) which maps reads from each sample to

174 pseudogenomes for both parent species (described below) to obtain a merged output
175 alignment file in order to alleviate reference bias associated with mapping hybrids to only a
176 single reference genome (Holt *et al.* 2013; Huang *et al.* 2014). For this approach, we mapped
177 reads for each individual to both a *P. sungorus* pseudogenome and a *P. campbelli*
178 pseudogenome with Hisat v.2.2.0 (Kim *et al.* 2019) with default settings and retaining at most
179 100 distinct, primary alignments, although multi-mapped reads were removed downstream
180 (described below). We generated the *P. sungorus* pseudogenome by mapping RNASeq reads
181 from a male *P. sungorus* individual (30.6 million total read pairs; NCBI SRA: SRR17223284;
182 Moore *et al.* 2022) to the *P. sungorus* reference genome (GCA_023856395.1) with bwa-mem
183 v.2.2.1 (Vasimuddin *et al.* 2019), and the *P. campbelli* pseudogenome by mapping female *P.*
184 *campbelli* whole genome sequencing reads (average coverage: 33x; NCBI SRA: SRR17223279;
185 Moore *et al.* 2022) to the *P. sungorus* reference genome. Because our *P. sungorus*
186 pseudogenome was based on a male hamster and the reference genome on a female hamster,
187 we excluded reads mapping to the PAR because sequences mapping to this region could have
188 originated from either the X or Y chromosomes and interfered with subsequent variant calling.
189 Following mapping, we used GATK v.4.2.5.0 HaplotypeCaller (-ERC GVCF) to call SNPs then
190 performed genotyping with genotypeGVCFs. We hard-filtered our SNPs (--mask-extension 5
191 "QD < 2.0" "FS > 60.0" "MQ < 40.0" "QUAL < 30.0" "DP < 10" "DP > 150") and restricted
192 SNPs to biallelic loci. Finally, we incorporated filtered SNPs back into the *P. sungorus*
193 reference genome with FastaAlternateReferenceMaker to create the *P. sungorus* and *P.*
194 *campbelli* pseudoreferences. For our RNASeq data, we appended query hit indexes to
195 resulting alignment files using hisat2Tophat.py (https://github.com/goodest-goodlab/pseudo-
196 it/tree/master/helper-scripts/hisat2Tophat.py, last accessed March 8th, 2022) to maintain
197 compatibility with the modtools pipeline. We used our VCFs (above) to generate a mod-file for
198 both species with vcf2mod from Lapels v.1.1.1 to convert alignments to the *P. sungorus*

199 reference genome, and Suspenders 0.2.6 to merge alignments while retaining the highest
200 quality alignment per read (Holt *et al.* 2013; Huang *et al.* 2014). We used featureCounts v.2.0.1
201 (Liao *et al.* 2014) to estimate counts of read pairs that aligned to the same chromosome (-B
202 and -C) and retained only singly-mapped reads. Summaries of properly mapped reads for each
203 sample can be found in Table S2.

204 We sought to compare the gene expression phenotypes observed in dwarf hamsters to
205 those previously documented in house mice using published RNASeq data for the same four
206 spermatogenic cell types of two subspecies of house mouse and their sterile F1 hybrids
207 (Larson *et al.* 2017; Hunnicutt *et al.* 2022). These studies examined two subspecies of house
208 mice, *Mus musculus musculus* (intra-subspecific F1 males between wild-derived inbred strains
209 PWK/PhJ♀ and CZECHII/EiJ♂) and *M. m. domesticus* (intra-subspecific F1 males between
210 wild-derived inbred strains WSB/EiJ♀ and LEWES/EiJ♂) and their sterile (PWK♀ x LEWES♂)
211 F1 hybrids for disrupted gene expression across spermatogenesis following the same FACS
212 protocols implemented in this study. For all comparisons between house mice and dwarf
213 hamsters, we used read count files generated previously for house mice (Hunnicutt *et al.* 2022)
214 and performed all subsequent analyses in parallel for both systems.

215

216 **Estimating nucleotide diversity and divergence within and between crosses and strains**
217
218 We next estimated nucleotide diversity within and divergence between each strain or
219 cross for parent species and hybrids (π and d_{XY}). We used the bam files generated above from
220 mapping each strain or cross to its respective reference genome (either GCA_023856395.1 for
221 dwarf hamsters or GRCm38.p6 for house mice) to call SNPs as described above but with the
222 addition of a step to split reads at intronic regions using the GATK function SplitNCigarReads.
223 We generated two VCFs, one for dwarf hamster crosses and the other for house mouse

224 crosses, which we processed and filtered separately. If an individual mouse or hamster was
225 sequenced for more than one cell type, we randomly chose one of the represented cell types
226 to be included in the analysis. We hard-filtered our SNPs as above and restricted SNPs to
227 biallelic loci. Because our SNPs were called from RNASeq data and thus may be susceptible to
228 allelic imbalances or coverage differences between samples, we next investigated how the
229 inclusion of SNPs with different levels of missing data impacted estimation of π and d_{XY}. We
230 used vcftools v.0.1.17 (Danecek *et al.* 2011) to filter SNPs allowing between 0% and 90%
231 missing data (--max_missing; Supplemental Figure S3), and filtered SNPs with a depth lower
232 than 5 and higher than 60 (~2-3 higher than average coverage) to eliminate multi-mapped
233 reads. Finally, we used pixy v.1.2.10.beta2 (Korunes and Samuk 2021) on our filtered VCFs to
234 estimate π and d_{XY}. Patterns of nucleotide diversity across strains and crosses were
235 qualitatively similar across missing data thresholds, so we present results corresponding to
236 10% missing data in the main text. However, we note that for all comparisons, estimates of π
237 and d_{XY} decreased with more stringent missing data thresholds regardless of strain or cross
238 (Supplemental Figure S3).
239
240 **Gene expression pre-processing**
241 Following read processing and mapping, we conducted all analyses in R v.4.3.1. We
242 classified genes as "expressed" if genes had a minimum of one Fragment Per Kilobase of exon
243 per Million mapped reads (FPKM) in at least three samples, resulting in 21,077 expressed
244 genes across the dwarf hamster dataset and 21,212 expressed genes across the house mouse
245 dataset. We also identified sets of genes "induced" in a given cell-type defined as genes with a
246 median expression in a given cell population (normalized FPKM) greater than two times its
247 median expression across all other sorted cell populations (following Kousathanas *et al.* 2014).
248 We calculated normalized FPKM values by adjusting the sum of squares to equal one using the

249 R package vegan v.2.6-4 (Oksanen *et al.* 2013). We conducted expression analyses using
250 edgeR v.3.42.4 (Robinson *et al.* 2010) and normalized the data using the scaling factor method
251 (Anders and Huber 2010).

252 We qualitatively assessed cell population purity both by visual inspection during cell
253 sorting and following sequencing by assessing the expression of a panel of marker genes
254 specific to the four cell populations targeted by our FACS protocol and present in only a single
255 copy in the *P. sungorus* annotation. Spermatogonia markers included *Dmrt1* (Raymond *et al.*
256 2000) and *Hells* (Green *et al.* 2018). Leptotene/zygotene markers included *Ccnb1ip1* and
257 *Adad2* (Hermann *et al.* 2018). Diplotene was characterized by *Aurka* and *Tank* expression
258 (Murat *et al.* 2023) and round spermatids by *Cabyr* and *Acrv1* expression (Green *et al.* 2018).
259 To estimate relative purity, we compared mean marker gene expression across replicates for a
260 given cell population for both parent species. A cell population was considered qualitatively
261 pure if it had higher marker gene expression than other populations isolated by our FACS
262 protocol and if X-linked gene expression matched the expected regulatory dynamics (*i.e.,*
263 active vs. silenced (MSCI) vs. repressed (PSCR); Handel 2004; Namekawa *et al.* 2006). We
264 examined expression patterns across cell populations for all genes, autosomal genes, and X-
265 linked genes using MDS plots generated with the plotMDS function in limma v.3.56.2 (Ritchie
266 *et al.* 2015) and heatmaps using ComplexHeatmap v.2.16.0 (Gu *et al.* 2016). MDS plots used
267 the top 500 genes with the largest fold change difference between samples.
268

269 **Differential gene expression analysis**

270 We assessed differential gene expression by contrasting hybrids and each parent
271 species for all cell populations. We fit the expression data for dwarf hamsters and house mice
272 separately with negative binomial generalized linear models with Cox-Reid tagwise dispersion
273 estimates and adjusted P-values to a false discovery rate (FDR) of 5% (Benjamini and

274 Hochberg 1995). We quantified the biological coefficient of variation (BCV), a metric
275 representing the variation in gene expression among replicates (McCarthy *et al.* 2012), for each
276 dataset. Additionally, we calculated the BCV of just parental males or hybrid samples for each
277 species for the first three cell populations to examine whether dwarf hamster hybrids exhibited
278 more variability in expression than house mouse hybrids and parental dwarf hamsters. For our
279 differential expression analyses, we contrasted expression between hybrids and each parent
280 so that a positive log fold-change (logFC) indicated overexpression in sterile males and
281 implemented a logFC cutoff of 1.25. We then categorized differentially expressed (DE) genes
282 into one of four categories: DE relative to only one parent species, DE relative to both parent
283 species but with intermediate expression (intermediate), and DE relative to both parent species
284 but outside of the range of either parent species (transgressive; Figure S2). Unless otherwise
285 specified, results discussed in the main text are restricted to transgressive DE genes and are
286 presented with the logFC from the contrast of the hybrid offspring to the parent with the same
287 X chromosome (*P. campbelli* for dwarf hamster F1 hybrids and *M. m. musculus* for house
288 mouse F1 hybrids). Transgressive DE genes have similar logFC values regardless of which
289 parent is used as the contrast, but figures depicting the logFC between F1 hybrids and *P.*
290 *sungorus* or *M. m. domesticus* are provided in supplementary material.

291 We tested for significant differences in the number of under and overexpressed
292 transgressive DE genes within a stage for both house mouse and hamster hybrids using X^2
293 tests with chisq.tests in R and used FDR correction for multiple comparisons. We also tested
294 for differences in the magnitude of misexpression between mouse and hamster hybrids for
295 each stage by comparing the distributions of logFC of transgressive DE genes between hybrids
296 and parent species using Wilcoxon signed-rank tests and FDR correction. To characterize
297 hybrid diplotene expression in both house mice and dwarf hamsters, we used two approaches.
298 First, we calculated Pearson's correlation coefficient *(r)* between average normalized hybrid

299 diplotene expression and the average normalized expression in each parental cell type. We
300 corrected p-values for each correlation with FDR. We generated bootstrap values for each
301 correlation coefficient by randomly sampling the expression matrices with replacement for
302 each sample type for 1000 replicates. Second, we compared the gene sets that escaped MSCI
303 in each species with gene sets that characterize stage-specific expression in parent species.
304 For this analysis, we defined sets of overexpressed X-linked diplotene genes as genes with
305 expression (normalized FPKM) in hybrids that was in the top 10% of X-linked genes in parental
306 diplotene samples (*i.e.,* genes that normally escape MSCI). We then compared these sets of
307 overexpressed hybrid diplotene genes to genes "induced" in each parental stage for each
308 species. We used gProfiler2 v.0.2.3 (Kolberg *et al.* 2020) in R to perform gene ontology (GO)
309 analysis to identify GO terms overrepresented in hybrid DE genes sets for each cell population.
310 We only included *P. sungorus* genes associated with mouse orthologs in our GO analysis (as
311 established by Moore *et al.* 2022), and for our background gene lists, we used *P. sungorus*
312 genes associated with mouse orthologs that were "expressed" in hybrids and both parent
313 species in a given stage. We retained only Biological Process GO terms with an FDR below
314 0.05 and ran gProfiler2 both with and without the highlight option, a two-stage algorithm for
315 reducing resulting GO terms by grouping significant terms into sub-ontologies and then
316 identifying the gene sets that give rise to other significant functions (Kolberg *et al.* 2020). To
317 test whether specific chromosomes were enriched or depleted for transgressive DE genes for a
318 given stage, we performed hypergeometric tests on the number of DE genes on a given
319 chromosome with phyper and adjusted P-values to an FDR of 5%. We also assessed overlap
320 in specific DE genes within stages between house mice and dwarf hamsters. We estimated
321 whether overlap was more or less than expected by chance using hypergeometric tests and
322 performed GO enrichment on overlapping genes.

323

324 **Characterizing the behavior of PAR genes in dwarf hamsters**

325 We sought to characterize the regulatory behavior of PAR genes in dwarf hamster
326 parent species and hybrids to determine if (1) PAR genes are normally silenced in parent
327 species (consistent with an extension of MSCI to the PAR) and (2) if PAR genes were
328 overexpressed in hybrids (consistent with disrupted MSCI in the PAR of hybrids). The PAR on
329 the *P. sungorus* X chromosome is on the distal arm of the X chromosome from around
330 115,350,000-119,112,095 bp (Moore *et al.* 2022). There are 15 annotated *P. sungorus* genes in
331 this region (Table S3), which is comparable to the latest PAR assembly in C57BL/6J house
332 mice (Kasahara *et al.* 2022). Six of these are orthologous to annotated genes in mice (*Tppp2*,
333 *Gprin1*, *Ndrg2*, *Kcnip4*, *Ndrg2*, and *Hs6st3*), but they are not located in the mouse PAR
334 (Kasahara *et al.* 2022). Only seven of the annotated genes in the PAR were expressed in more
335 than three replicates across all samples (Psun_G000022875, Psun_G000022880,
336 Psun_G000022883, Psun_G000022886, *Tppp2*, *Gprin1*, and *Ndrg2*). For these genes, we
337 assessed whether these genes were consistently expressed or silenced in parent species at
338 any cell stage and whether any genes were differentially expressed between hybrids and either
339 species.

340 **RESULTS**

341 **Impaired sperm production in hybrid male dwarf hamsters**

342 We first established the extent of hybrid male sterility in dwarf hamsters by comparing
343 reproductive phenotypes for *P. campbelli*, *P. sungorus*, and F1 hybrid males (Figure 1; Table
344 S1). *Phodopus sungorus* males had smaller testes and seminal vesicles than *P. campbelli*
345 males (Dunn's Test relative testes weight $p < 0.001$; relative seminal vesicle weight $p = 0.0061$;
346 Figure 1). These differences are qualitatively consistent across independent laboratory colonies

(Ishishita *et al.* 2015; Bikchurina *et al.* 2018) and likely reflect species-specific differences between *P. campbelli* and *P. sungorus*. *Phodopus sungorus* males also had lower nucleotide diversity (π = 0.00013) than *P. campbelli* males (π = 0.00045) and both house mouse parental crosses between fully inbred mouse strains (*M. m. musculus* π = 0.00029; *M. m. domesticus* π 0.00017; Figure S3), which could contribute to depression of male fertility within this highly inbred laboratory colony (Brekke *et al.* 2018). Nucleotide divergence between parental dwarf hamster species was elevated relative to house mice (d_{xy} = 0.0020 vs. 0.0010), consistent with reported older divergence time estimates for dwarf hamsters (Neumann *et al.* 2006). However, these dwarf hamster species did not differ in normalized sperm counts ($p = 0.071$) or in sperm motility ($p = 0.12$). The F1 hybrid males exhibited extreme reproductive defects relative to *P. campbelli* (Figure 1). Hybrid males had smaller testes ($p < 0.001$) and seminal vesicles ($p < 0.001$) than male *P. campbelli* hamsters, and importantly, produced almost no mature spermatozoa. In the one instance where a hybrid male produced a single mature spermatozoon, it was non-motile, indicating severe reproductive impairment in hybrid males. Overall, our results confirmed previous reports of reduced fertility in hybrid male dwarf hamsters (Ishishita *et al.* 2015; Bikchurina *et al.* 2018).

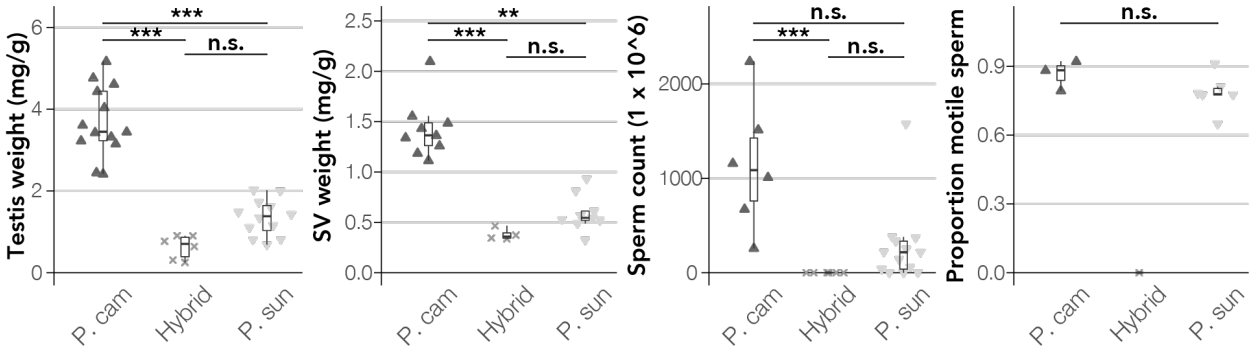

Figure 1. Evidence of some hybrid male sterility in dwarf hamsters. We assessed paired testes weight and paired seminal vesicle weight (SV; both normalized by body weight), sperm

count, and proportion of motile sperm for *P. sungorus*, *P. campbelli*, and F1 hybrids. Whiskers extend to either the largest or smallest value or no further than 1.5 times the interquartile range, and *** indicates $p < 0.001$, ** indicates $p < 0.01$, and n.s. indicates non-significant difference between means at $p > 0.05$ using a post-hoc Dunn's test with FDR correction. Upwards-pointing triangles (▲) indicate *P. campbelli*, downwards-pointing triangles (▼) indicate *P. sungorus*, and crosses (✖) indicate F1 hybrids.

Cell-specific gene expression across spermatogenesis

To characterize cell-specific gene expression, we used FACS to isolate enriched cell populations from each fertile parent species and their sterile F1 hybrids across four stages of spermatogenesis. The four targeted populations included: spermatogonia (mitotic precursor cells), leptotene/zygotene spermatocytes (meiotic cells before MSCI), diplotene spermatocytes (meiotic cells after MSCI), and round spermatids (postmeiotic cells). We were unable to isolate round spermatids from the F1 hybrids, which was consistent with the lack of mature spermatozoa present in the cauda epididymis extractions (Figure 1). We sequenced RNA from each cell population for *P. campbelli* (spermatogonia n = 4, leptotene/zygotene n = 5, diplotene n = 5, and round spermatids n = 4; Table S2), *P. sungorus* (spermatogonia n = 4, leptotene/zygotene n = 4, diplotene n = 5, and round spermatids n = 3), and F1 hybrid males (*P. campbelli* ♀ x *P. sungorus* ♂; spermatogonia n = 4, leptotene/zygotene n = 4, diplotene n = 4). We compared our hamster expression data to an analogous cell-specific RNASeq dataset from two species of house mice, *Mus musculus musculus* and *M. m. domesticus*, and their sterile F1 hybrids (n = 3 for all cell populations in each cross; Larson *et al.* 2017).

We used two approaches to qualitatively evaluate the purity of spermatogonia, leptotene/zygotene spermatocytes, diplotene spermatocytes, and round spermatids isolated

391 from males from both parental species: (1) we quantified the relative expression of a panel of
392 cell population marker genes, and (2) we characterized the expression patterns of the sex
393 chromosomes across development. We found that our candidate marker genes had the
394 highest expression in their expected cell population for all stages except leptotene/zygotene
395 (Figures S4 and S5), indicating high purity of spermatogonia, diplotene spermatocytes, and
396 round spermatids. Leptotene/zygotene markers did not have the highest expression in
397 leptotene/zygotene samples (except for *Ccnb1ip1*), potentially indicating lower purity of this
398 cell population. Nonetheless, the patterns of X chromosome expression in fertile parents were
399 consistent with expectations across this developmental timeline: the X chromosome had active
400 expression in spermatogonia and leptotene/zygotene cells, was inactivated in diplotene cells
401 consistent with MSCI, and was partially inactivated in round spermatids, consistent with PSCR
402 (Figure 2; Namekawa *et al.* 2006), indicating successful isolation of these cell populations.
403 When we examined overall expression differences within dwarf hamsters and within
404 house mice, we found that samples clustered primarily by cell population on MDS1 and 2
405 (Figure 3), then by cross/strain when cell populations were examined separately (Figures S6
406 and S7). Within all cell populations across both systems, hybrids showed intermediate overall
407 expression patterns to parent species (Figures S6 and S7). However, in dwarf hamsters but not
408 house mice, spermatogonia and leptotene/zygotene samples overlap rather than forming
409 distinct clusters (Figure 3). Further, the expression profiles of hybrid diplotene cells ranged
410 from clustering with parental leptotene/zygotene to parental diplotene cells, which contrasted
411 with what we observed in house mice where hybrid diplotene cells clustered distinctly with
412 parental diplotene cells (Figure 3). Overall, our results indicate that we successfully isolated cell
413 populations in dwarf hamsters that span key stages of spermatogenesis.
414

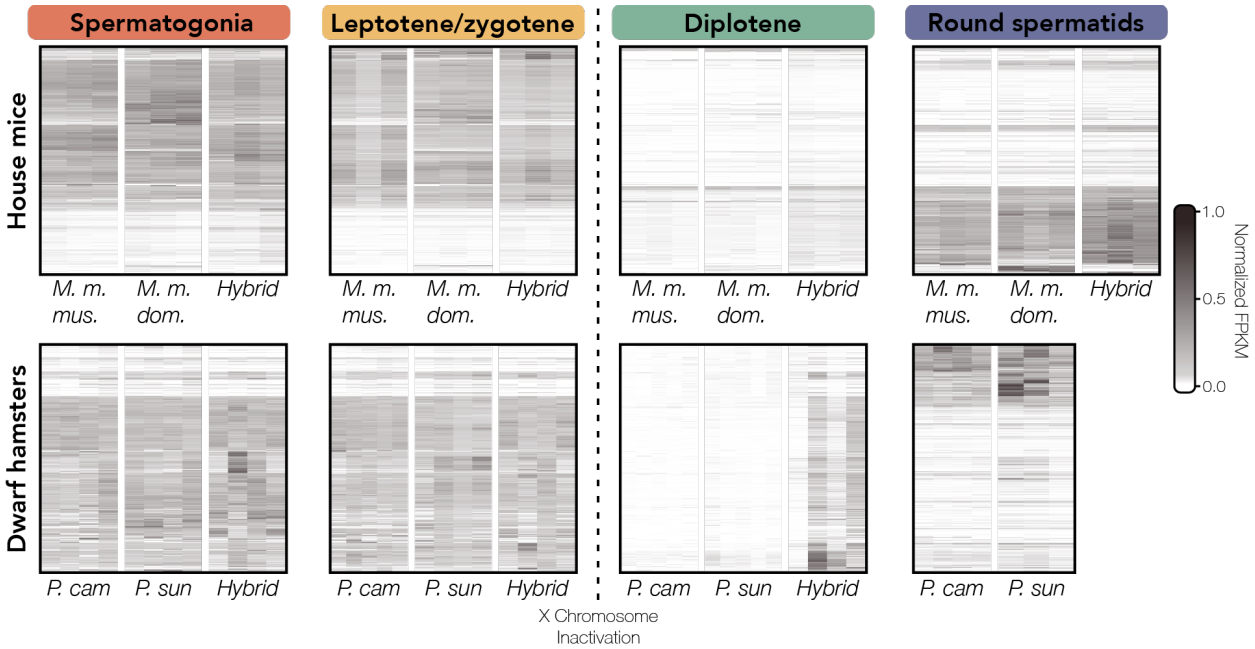

415

416 **Figure 2. Overexpression of X-linked genes in diplotene spermatocytes in both house**

417 **mouse and dwarf hamster hybrids.** Heatmap of X-linked gene expression in house mice

418 (upper panel) and dwarf hamsters (lower panel) plotted as normalized FPKM values that are

419 hierarchically clustered using Euclidean distance. Each column represents a different

420 individual, each row represents a gene, and darker colors indicate higher expression. The

421 heatmap was generated with the R package ComplexHeatmap v.2.12.0 (Gu et al. 2016). Note,

422 hybrid dwarf hamsters do not produce mature spermatozoa, and accordingly, we were unable

423 to isolate round spermatids.

424

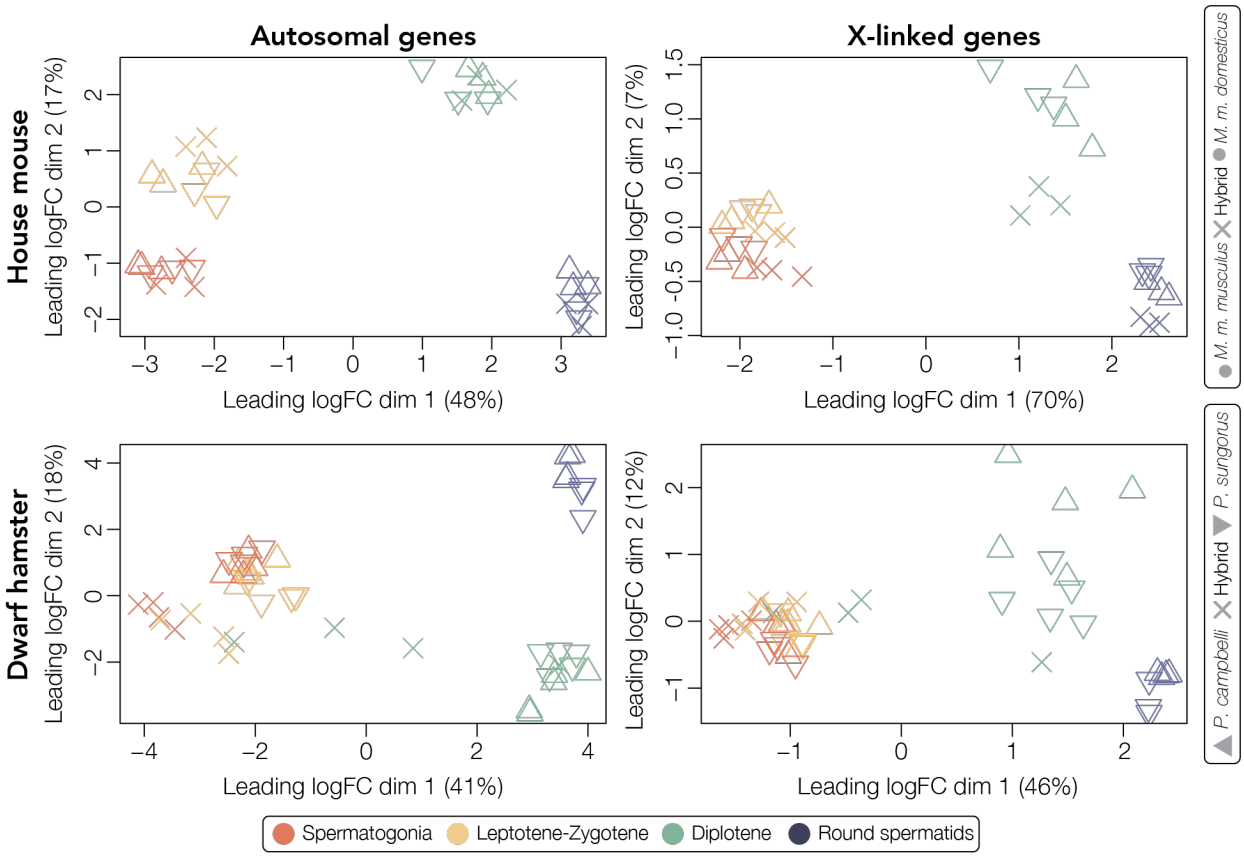

Figure 3. Hybrid gene expression profiles cluster by parental spermatogenic cell population in house mice but not dwarf hamsters. Multidimensional scaling (MDS) plots of distances among house mouse (upper panels) and dwarf hamster (lower panels) samples for expressed autosomal (left) and X-linked (right) genes. Distances are calculated as the root-mean-square deviation (Euclidean distance) of log2 fold changes among the top 500 genes that distinguish each sample. Each strain or cross is indicated by a symbol, and samples are colored by cell population.

Disrupted transcription early in spermatogenesis in dwarf hamsters

We sought to characterize which expression phenotypes were associated with sterile hybrids in both house mice and dwarf hamsters. We first investigated whether differential gene expression in hybrids tended towards intermediate or transgressive expression, and then within transgressive DE genes, whether misexpression tends towards up- or downregulation in

438 hybrids compared to parents. Differential gene expression in mouse hybrids had a slight bias
439 towards transgressive expression except in round spermatids (percentage of transgressive DE
440 genes: SP: 72.0%, LZ: 62.7%, DIP: 60.8%, and RS: 24.9%; Figures 4B and S2), while almost
441 all differential expression in dwarf hamster hybrids was transgressive (percentage of
442 transgressive DE genes: SP: 99.2%, LZ: 98.0%, and DIP: 97.1). For transgressive DE genes,
443 autosomal misexpression in hybrid house mice was biased towards upregulation across
444 spermatogenesis (mean logFC of spermatogonia autosomal DE genes: +1.90/ X^2: $p < 0.001$;
445 leptotene/zygotene: +1.33/ X^2: $p < 0.001$; diplotene: +0.47/ X^2: $p < 0.001$; Figures 4C and S8),
446 as was X-linked misexpression (spermatogonia mean logFC: +1.98 / X^2: $p < 0.001$;
447 leptotene/zygotene: +2.50/ X^2: $p < 0.001$; diplotene: +2.78/ X^2: $p < 0.001$). In contrast, we found
448 that the direction of misexpression in dwarf hamster hybrids was stage-specific. Autosomal DE
449 genes in dwarf hamster hybrids were overwhelmingly downregulated in both early stages of
450 spermatogenesis, especially in comparison to house mice (mean logFC of spermatogonia
451 autosomal DE genes: -4.38/ X^2: $p < 0.001$; leptotene/zygotene: -4.67/ X^2: $p < 0.001$; Figure 4D)
452 but upregulated in diplotene (average logFC = +4.67/ X^2: $p < 0.001$; Figures 4D and S8). When
453 comparing both X-linked and autosomal expression in dwarf hamsters, we found similar
454 patterns: almost all X-linked DE genes in the first two stages of spermatogenesis were
455 exclusively downregulated (spermatogonia mean logFC = -6.57/ X^2: $p < 0.001$;
456 leptotene/zygotene: -6.73/ X^2: $p < 0.001$), but misexpression was biased towards upregulation
457 in diplotene (mean logFC: 5.70/ X^2: $p < 0.001$).

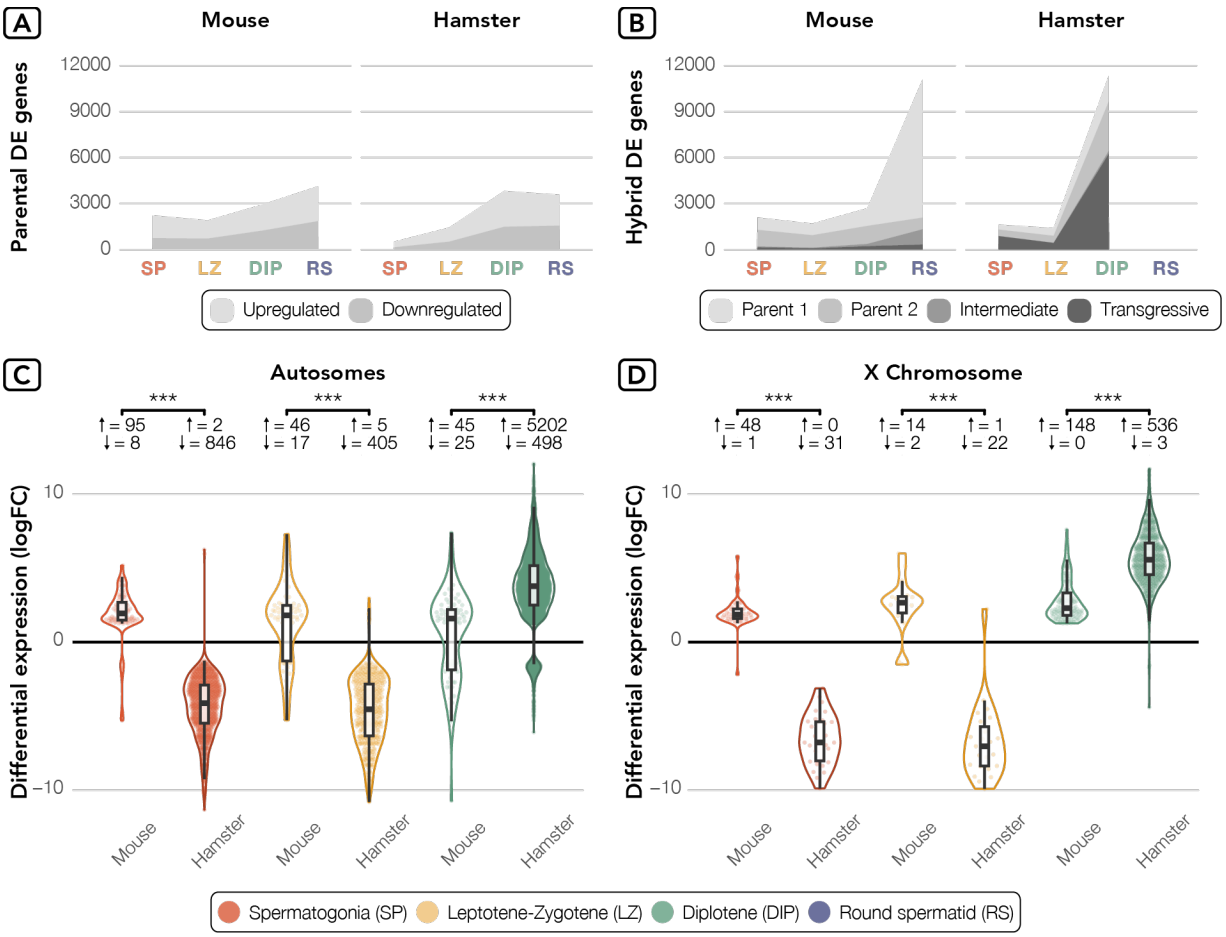

Figure 4. House mice and dwarf hamster hybrids have opposite patterns of disrupted regulation early in spermatogenesis. A. Up- and down-regulated DE genes between parent species for house mice (left; *M. m. musculus* vs. *M. m. domesticus*) and dwarf hamsters (right; *P. sungorus* vs. *P. campbelli*). **B**. Counts of DE genes between hybrids and one parent species (two lightest shades of gray where Parent 1 was either *M. m. musculus or P. sungorus* and parent 2 was either *M. m. domesticus* or *P. campbelli)* or between hybrids and both parents (two darker shades of gray) that showed either intermediate or transgressive expression. **C.** Transgressive DE genes in house mouse and dwarf hamster hybrids for autosomal genes where the logFC represents hybrid expression relative to *M. m. musculus* or *P. campbelli,* respectively, and **D.** transgressive DE gene expression for X-linked genes. Results are displayed for autosomes (left) and the X chromosome (right). *** indicates $p < 0.001$ for

470 pairwise comparisons from Wilcoxon signed-rank tests after FDR correction. Whiskers extend
471 to either the largest or smallest value or no further than 1.5 times the interquartile range. The
472 number of up and downregulated DE genes in hybrids are listed next to arrows indicating
473 direction of differential expression.
474
475 Second, we investigated how developmental stage influenced the extent of hybrid
476 misexpression. In both systems, the number of DE genes between parent species increased
477 with the progression of spermatogenesis, consistent with less constraint on gene expression
478 levels as spermatogenesis progresses (Figure 4A; Kopania *et al.* 2022a; Murat *et al.* 2023).
479 Similarly, transgressive misexpression in both hybrid dwarf hamsters and house mice
480 increased with the progression of spermatogenesis, though to a greater extent in dwarf
481 hamsters (Figure 4B). While both parental DE genes and transgressive hybrid DE genes
482 increased with the progression of spermatogenesis, parental DE genes initially exceeded the
483 number of transgressive hybrid DE genes in hybrids in spermatogonia and leptotene/zygotene
484 spermatocytes. However, in diplotene spermatocytes, transgressive hybrid differential
485 expression surpassed parental differential expression in both house mice and dwarf hamsters.
486 We also found a much greater genome-wide disruption of expression in diplotene cells of
487 hybrid dwarf hamsters than in hybrid house mice (Figures 4C-D and S8-S10), indicating more
488 widespread regulatory disruption. We then compared transgressive DE genes between house
489 mice and dwarf hamster hybrids across all three stages and found that the number of shared
490 DE genes did not differ from the number expected by chance (spermatogonia = 3 genes,
491 hypergeometric test $p = 0.98$; leptotene/zygotene = 2 genes, $p = 0.59$; and diplotene = 78
492 genes, $p = 0.18$; Table S4). These sets of shared DE genes between house mice and dwarf
493 hamsters were not significantly enriched for any GO terms, although many play known roles in
494 spermatogenesis, the apoptotic process, and cell differentiation (Table S5) and may be

495 promising candidates for future functional analysis. Ultimately, we found that, although few
496 specific genes have similarly disrupted expression in dwarf hamster and house mouse hybrids,
497 there are similar trends in the patterns of transgressive expression across stages in both
498 systems.

499 To determine if the differences we observed in the extent of misexpression between
500 dwarf hamsters and house mice was due to greater expression variability across our dwarf
501 hamster samples, we calculated the BCV, a measurement of inter-replicate variability, for each
502 species and hybrid across the first three cell populations. Inter-replicate variability was higher
503 in dwarf hamster hybrids relative to house mouse hybrids (dwarf hamster BCV = 0.69; house
504 mice = 0.18). Additionally, nucleotide diversity within dwarf hamster hybrids was higher (π =
505 0.0012) than within house mouse hybrids (π = 0.00052; Figure S3). However, the extent of the
506 expression variability observed in hybrids relative to the inter-replicate variability of parental
507 species differed between house mice and dwarf hamsters: dwarf hamster hybrid variability was
508 more than dwarf hamster parental samples (*P. campbelli* = 0.49; *P. sungorus* = 0.40), but
509 hybrid variability was similar to parental samples for house mice (*M. m. musculus* = 0.19; *M. m.*
510 *domesticus* = 0.22). The greater inter-replicate expression variability in dwarf hamster hybrids
511 relative to parent species suggests that the increased misexpression we see in hybrids cannot
512 be explained by greater inter-replicate variability in our dwarf hamster samples alone, and it
513 may also reflect the greater nucleotide diversity present among dwarf hamster hybrids.

514 Third, we characterized whether there was a clear difference between the autosomes
515 and sex chromosomes in expression phenotype by testing whether the X chromosome was
516 enriched for transgressive DE genes in each stage for both systems. Across all stages of
517 spermatogenesis in house mice, the X chromosome was enriched for transgressive DE genes
518 between hybrids and parents (spermatogonia $p < 0.001$; leptotene/zygotene $p < 0.001$;
519 diplotene $p < 0.001$; round spermatids $p < 0.0036$; Figure S9). In contrast, misexpression in

520 dwarf hamsters was not uniformly sex chromosome-specific across all stages, as the sex
521 chromosomes in dwarf hamsters showed no enrichment for transgressive DE genes early in
522 spermatogenesis (spermatogonia: $p = 0.21$; Figure S10) despite X chromosome enrichment in
523 both leptotene/zygotene ($p = 0.0064$) and round spermatids ($p < 0.001$). However, we note that
524 the magnitude of misexpression was greater for sex chromosomes than autosomes in dwarf
525 hamsters across all stages (Figures 4C and 4D; discussed above). Only two autosomes were
526 enriched for transgressive DE genes in dwarf hamsters in any cell population: one scaffold on
527 chromosome 5 in spermatogonia (JAJQIY010003390.1; hypergeometric test; $p = 0.003$) and
528 chromosome 11 in leptotene/zygotene ($p = 0.017$; Figure S10). Together, the subtle differences
529 in the distribution of transgressive DE genes across autosomes and the X chromosome
530 between dwarf hamster hybrids and house mouse hybrids suggest a difference in the extent of
531 the role for sex chromosome-specific disruption between systems.
532

533 **Misexpression in diplotene appears to be unrelated to disrupted MSCI in dwarf hamsters**

534 We next asked whether expression patterns indicated similar disrupted regulatory
535 processes resulting in sex chromosome-specific misexpression in both systems. In sterile
536 hybrid house mice, the mean logFC of transgressive X-linked DE genes during diplotene was
537 higher than the mean logFC of transgressive autosomal DE genes (+0.47 in contrast to +2.78;
538 Figure 4C and D), consistent with disrupted MSCI (Good *et al.* 2010; Bhattacharyya *et al.* 2013;
539 Campbell *et al.* 2013; Turner and Harr 2014; Larson *et al.* 2017, 2022). In sterile dwarf hamster
540 hybrids, we also found elevated mean logFC of transgressive DE X-linked genes relative to
541 autosomal genes (+3.69 in contrast to +5.70), but the extent of X chromosome overexpression
542 was greater than in hybrid house mice (Figures 2, 4C, and 4D). There was also more variability
543 in the relative extent of overexpression of X-linked genes in hybrid dwarf hamsters during
544 diplotene compared to the mean expression of X-linked genes of parental dwarf hamsters

545 (relative overexpression = 18.5 +/- 6.8) compared to hybrid house mice (relative overexpression
546 = 1.75 +/- 0.09; Figures 2 and S11). Strikingly, some hybrid male dwarf hamsters had an
547 almost completely silenced X chromosome, while others had an almost completely
548 transcriptionally-activated X chromosome (Figure 2).

549 Despite overexpression of the X chromosome during diplotene in hybrid dwarf
550 hamsters, the overall expression phenotype, including the identity and the extent of
551 misexpression of overexpressed genes, appeared to fundamentally differ between house
552 mouse and dwarf hamster hybrids (Figures 2 and 5A-5C). We established these differences in
553 X-linked overexpression using two approaches. First, we tested which parental cell types had
554 the highest expression correlation with hybrid diplotene cell types for both X-linked and
555 autosomal genes. In mice, the expression profile of X-linked genes in hybrids during diplotene
556 was most positively correlated with the expression profile of X-linked parental round spermatid
557 genes, consistent with disrupted MSCI (spermatogonia *(r)* = -0.25, $p < 0.001$;
558 leptotene/zygotene *(r)* = -0.073, $p = 0.035$; round spermatid *(r)* = 0.26, $p < 0.001$; Figures 2 and
559 5A). Autosomal diplotene genes showed no positive correlations with either spermatogonia (r =
560 -0.26; $p < 0.001$), leptotene/zygotene (r = -0.032; $p < 0.001$), or round spermatids (r = -0.060; p
561 < 0.001; Figure 5A). If the X-linked overexpression phenotype in dwarf hamsters was
562 consistent with disrupted MSCI, then we would also expect X-linked and autosomal expression
563 profiles in hybrid diplotene to follow the same patterns. In contrast to this prediction, hybrid
564 dwarf hamster diplotene expression profiles for both X-linked and autosomal genes had a
565 positive correlation with parental leptotene/zygotene (autosomal *(r)* = 0.14, $p < 0.001$; X-linked
566 *(r)* = 0.22, $p < 0.001$) and spermatogonia (autosomal *(r)* = 0.027, $p < 0.001$; X-linked *(r)* = 0.091,
567 $p = 0.016$) and a negative correlation with round spermatids (autosomal *(r)* = -0.30, $p < 0.001$;
568 X-linked *(r)* = -0.31, $p < 0.001$; Figure 5B). These striking differences in the strength and
569 direction of expression profile correlations suggest that the regulatory mechanisms underlying

570 the overexpression phenotype of X-linked genes in sterile hybrids differed between house mice
571 and dwarf hamsters.

572 This difference in pattern was further supported when we compared which sets of
573 genes were overexpressed in hybrid diplotene in dwarf hamsters and house mice. For this
574 approach, we looked at parental gene expression patterns to characterize which stages of
575 spermatogenesis all genes were normally active during and characteristic of (*i.e.,* "induced";
576 see Methods). Using this information, we then identified which X-linked genes were
577 overexpressed in hybrid diplotene (defined as genes with normalized expression in the top
578 10% of X-linked genes) and assessed which parental stages the overexpressed X-linked genes
579 were characteristic of in both systems. As in our correlation analysis, we found that in hybrid
580 house mice, the genes that were overexpressed in diplotene most closely resembled genes
581 that are normally active in round spermatids in parental mice (51.6% of genes), but that in
582 hybrid dwarf hamsters, overexpressed diplotene genes resembled spermatogonia- and
583 leptotene/zygotene-specific genes (47.6% and 41.6% respectively; Figure 5C). Because of the
584 dissimilarity in the genes that were overexpressed during diplotene in both systems, we next
585 performed gene ontology (GO) enrichment analyses on the set of transgressive DE genes in
586 hybrids to determine which biological processes could be potentially contributing to this
587 pattern. In contrast to house mice hybrids where transgressive DE genes were enriched for no
588 biological processes, the transgressive DE genes in dwarf hamster were enriched for several
589 biological processes including cell junction/extracellular matrix organization, system
590 development, inflammatory response, and apoptotic process which together point to
591 widespread disruption of numerous processes necessary for normal male fertility (highlighted
592 terms presented in Figure 5D and the full lists in Tables S6-S8). Collectively, these results
593 suggest that the X-linked overexpression phenotype in sterile hybrid dwarf hamsters is

inconsistent with disrupted MSCI and is possibly related to a stalling and breakdown of spermatogenesis between leptotene/zygotene and diplotene during Prophase I.

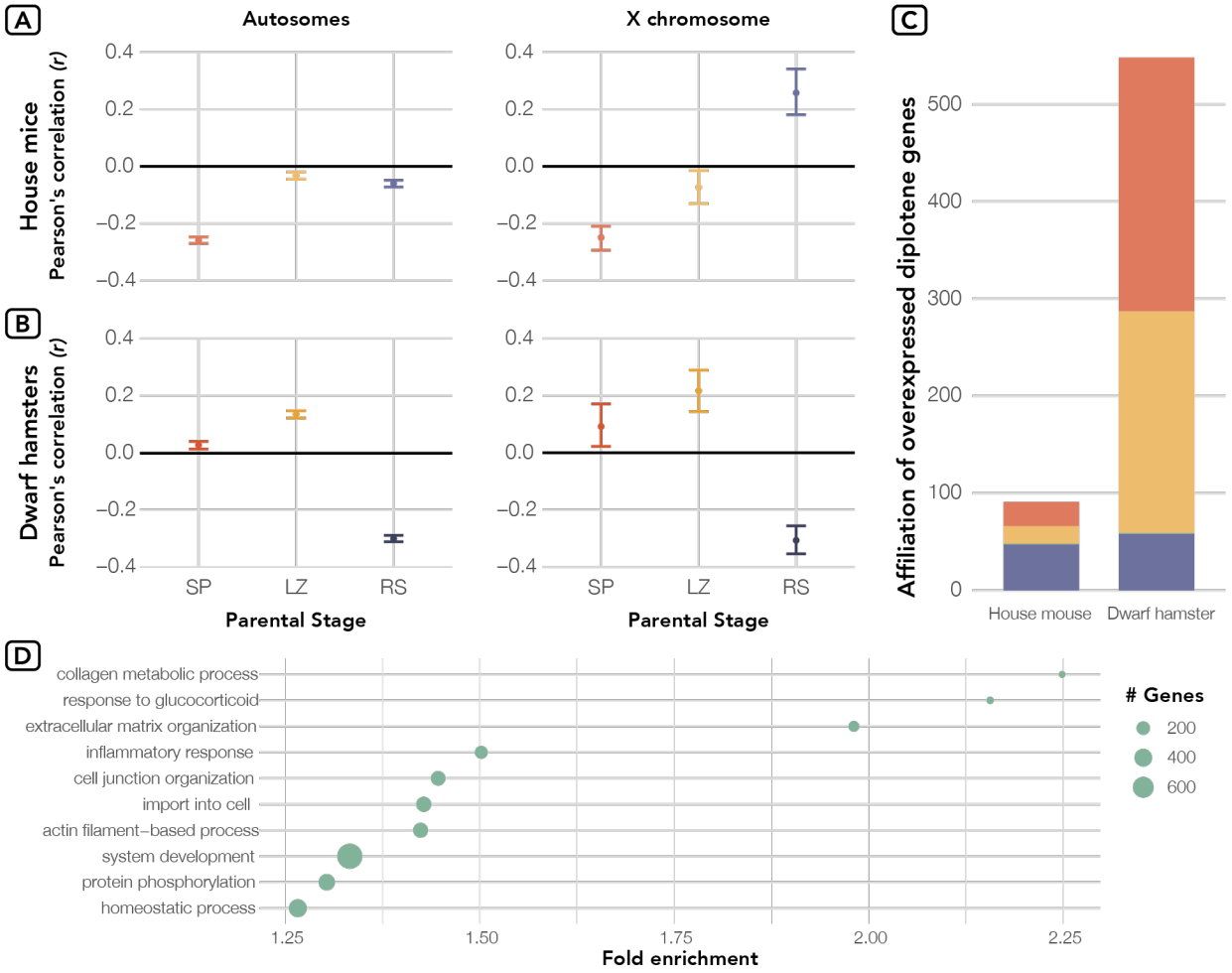

Figure 5. Spermatogenesis in hybrid dwarf hamsters appears to stall after leptotene/ zygotene. A. We calculated the Pearson's correlation coefficient *(r)* between mean hybrid diplotene expression and the mean expression for each parental cell type for both house mice and **B.** dwarf hamsters. Correlation coefficients were calculated for both autosomal (left panels) and X-linked (right panels) genes. We then generated bootstrap values by randomly sampling the expression matrices for 1000 replicates. All correlation coefficients were significantly different from zero ($p < 0.05$) after FDR correction. **C.** Classification of X-linked overexpressed

genes in diplotene cells of hybrid mice and dwarf hamsters by parental stage in which genes are induced. Genes are colored by cell type (red = spermatogonia, yellow = leptotene/zygotene, green = diplotene, and blue = round spermatids). **D.** Select enriched Biological Process GO terms (ranked by FDR) for transgressive DE genes between hybrid dwarf hamsters and *P. campbelli* in diplotene spermatocytes. Included terms shown are the result of the highlight function within gProfiler2 which collapses GO terms in a two-step clustering algorithm (Kolberg *et al.* 2020). Point size corresponds to the number of genes belonging to each GO term, and terms are plotted by the fold enrichment of the GO term in the dataset relative to the provided gene backgrounds.

PAR expression was not disrupted in sterile hybrid dwarf hamsters

Finally, we tested the hypothesis that hybrid sterility in dwarf hamsters may be correlated with asynapsis of the X and Y chromosomes because of divergence in the pseudoautosomal region (PAR) which prevents proper chromosome pairing (Bikchurina *et al.* 2018). The PAR is the only portion of the sex chromosomes that is able to synapse during routine spermatogenesis, and PAR genes are assumed to escape silencing by MSCI (Raudsepp and Chowdhary 2015). However, because XY asynapsis is common in dwarf hamster hybrids, Bikchurina et al. (2018) hypothesized that MSCI may extend to the PAR of hybrid male dwarf hamsters, resulting in the silencing of PAR genes in hybrids that may be critical to meiosis (Figure 6A). To test this hypothesis, we compared the expression of genes located in the dwarf hamster PAR (Moore et al. 2022) between parental dwarf hamster species and hybrid offspring across the timeline of spermatogenesis. Specifically, we hypothesized that if XY asynapsis results in an extension of MSCI to the PAR in hybrid dwarf hamsters, then hybrids should have similar PAR gene expression to parents early in meiosis before homologous chromosome synapse during pachytene. This should be followed by the silencing

630 of PAR genes in hybrids, but not parent species, during diplotene. If XY asynapsis does not
631 alter the regulation of the PAR in hybrids, then we may see two possible patterns. First, if all
632 PAR genes are critical to the later stages of spermatogenesis, then PAR genes in both hybrids
633 and parents should be uniformly expressed in diplotene. Alternatively, if PAR genes are not
634 critical to the later stages of spermatogenesis, then hybrids and parent species should have
635 similar PAR gene expression, and not all PAR genes may be expressed during diplotene.
636 We did not find evidence supporting PAR-wide silencing in dwarf hamster hybrids
637 during diplotene suggesting that MSCI is not extended to the PAR in dwarf hamster hybrids
638 because of XY asynapsis (Figure 6B). Furthermore, we do not see PAR-wide expression of
639 genes during diplotene in hybrids or parents, indicating that not all PAR genes are critical to
640 the progression of spermatogenesis in dwarf hamsters. In general, most PAR gene expression
641 followed similar trends between hybrids and parent species. Two PAR genes were differentially
642 expressed between hybrids and *P. campbelli* during diplotene (*Ndrg2* and Psun_G000022883;
643 Table S3), but these genes were still expressed in hybrids. Further, an association between
644 PAR misregulation during the early stages of spermatogenesis and hybrid male sterility also
645 seems unlikely as only one gene, *Gprin1*, showed transgressive differential expression in early
646 meiosis between both parent species and hybrids (Table S3). Thus, based on the current
647 annotation of the PAR in *P. sungorus*, we currently find no direct evidence linking improper
648 silencing of PAR genes to hybrid male sterility in dwarf hamsters.
649
650

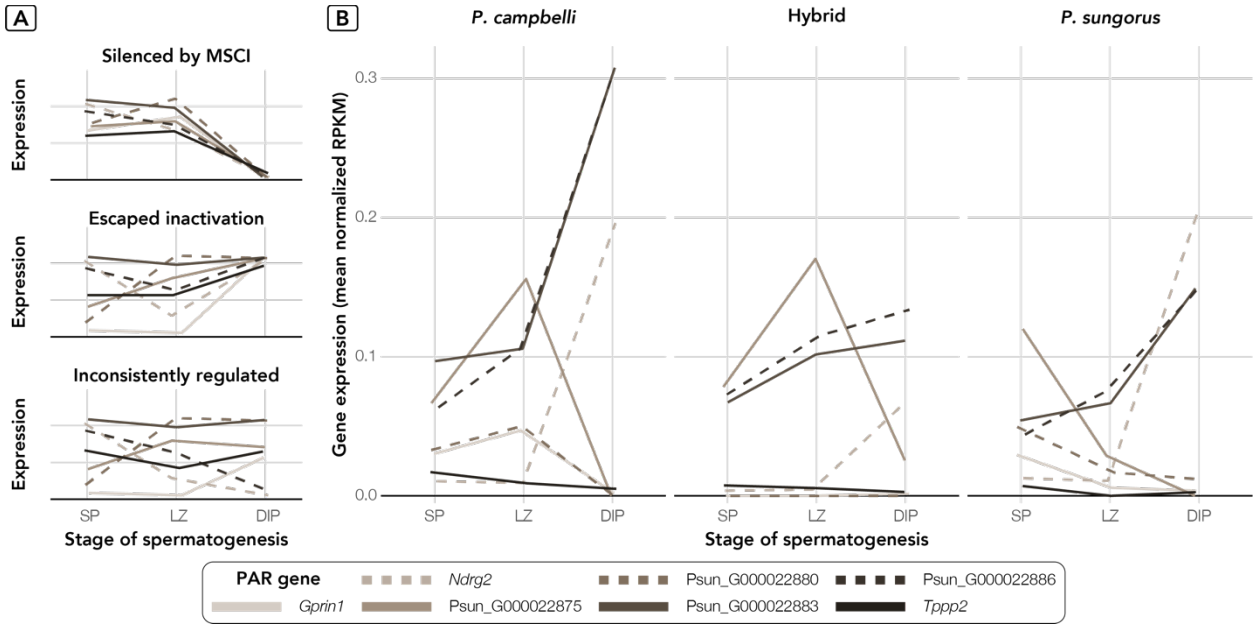

651

652 **Figure 6. PAR gene expression is not disrupted during spermatogenesis in hybrid dwarf**
653 **hamsters. A.** Hypothesized types of PAR gene expression across spermatogenesis. If MSCI
654 extends to the entire X chromosome, then PAR genes would show some level of expression
655 early in spermatogenesis which would then drop to zero in diplotene when MSCI occurs. If the
656 PAR escapes silencing by MSCI and if PAR genes are critical to spermatogenesis, then we
657 would expect PAR genes to be uniformly expressed in diplotene when the rest of the X
658 chromosome is silenced. Finally, if the PAR escapes silencing by MSCI but all PAR genes are
659 not critical to spermatogenesis, then we would expect some PAR genes to be expressed and
660 some to be not expressed in diplotene. **B.** Observed patterns of PAR gene expression (as
661 mean normalized RPKM across individuals) in parental species and hybrid dwarf hamsters for
662 all PAR genes (indicated by line type and color) across spermatogenesis (SP = spermatogonia,
663 LZ = leptotene/zygotene, and DIP = diplotene).

664

DISCUSSION

We used a comparative approach to understand common gene expression phenotypes associated with hybrid male sterility in two divergent rodent crosses. We characterized the asymmetry in the expression patterns of transgressive genes, how misexpression changed over developmental timelines, and how the X chromosome and autosomes differed in both of these aspects. We found that while there were similarities in hybrid expression phenotypes in house mice and dwarf hamsters, there were also differences in the timing and chromosomal distribution of disrupted gene expression that point towards different underlying mechanisms behind hybrid male sterility.

Asymmetry and developmental timing of misexpression in hybrids

We first investigated patterns of gene misexpression in sterile male hybrids. Studies of transgressive misexpression in sterile or inviable hybrids have often focused on whether hybrid expression is biased towards over or underexpression, with the hypothesis that expression may be biased towards overexpression if hybrid incompatibilities disrupt repressive gene regulatory elements (Meiklejohn *et al.* 2014; Barreto *et al.* 2015; Larson *et al.* 2017). In house mice, there is strong support for overexpression of both autosomal and X-linked genes in sterile F1 hybrids (Mack *et al.* 2016; Larson *et al.* 2017, 2022; Hunnicutt *et al.* 2022), and further work has shown that F1 hybrid expression patterns depend on both autosomal background and sex chromosome mismatch (Kopania *et al.* 2022b). Surprisingly, we found that in dwarf hamster hybrids, there was nearly uniform downregulation of transgressive DE genes in mitotic cells and early meiotic cells, suggesting that a loss of regulatory repression is not an inevitable outcome of hybrid genomes. Asymmetric patterns of misexpression have been found in many hybrids, including underexpression in sterile *Drosophila* hybrids (Michalak and Noor 2003;

689 Haerty and Singh 2006; Llopart 2012) and sterile introgression lines of tomato (Guerrero *et al.*
690 2016) and *Drosophila* (Meiklejohn *et al.* 2014), but overexpression has also been found in other
691 sterile hybrids (Llopart 2012; Davis *et al.* 2015). The variation we and others have found in
692 hybrid expression phenotypes suggests that the mechanisms of disrupted expression are
693 complex, even within groups with relatively shallow divergence times (such as rodents), and we
694 need more data from diverse hybrid sterility systems to begin to understand common drivers of
695 transgressive hybrid misexpression.

696 The downregulation we observed in early spermatogenesis in hybrid dwarf hamsters
697 could be due to impaired transcription factor binding with promoter or enhancer elements (Oka
698 *et al.* 2014; Guerrero *et al.* 2016) or disrupted epigenetic silencing. Disruption of epigenetic
699 regulation of gene expression has been increasingly linked to hybrid dysfunction in plants
700 (Shivaprasad *et al.* 2012; Lafon-Placette and Köhler 2015; Zhu *et al.* 2017), especially
701 polyploids (Paun *et al.* 2007), and may also contribute to hybrid male sterility in *Drosophila*
702 (Bayes and Malik 2009) and cattle x yak hybrids (Luo *et al.* 2022). At least one known
703 chromatin difference, an expansion of the heterochromatin-enriched Xp arm of the X
704 chromosome, has been documented between parental dwarf hamster species (Gamperl *et al.*
705 1977; Haaf *et al.* 1987). However, it is unknown what the functional consequences of this
706 chromatin state divergence or other diverged epigenetic regulatory mechanisms, such as
707 methylation, may be in hybrid dwarf hamster spermatogenesis, and further work is needed to
708 distinguish between potential mechanisms underlying the observed genome-wide
709 downregulation.

710 Spermatogenesis as a developmental process may be sensitive to disruption (Lifschytz
711 and Lindsley 1972; Wu and Davis 1993), but it remains an open question whether specific
712 stages of spermatogenesis, or developmental processes more broadly, may be more prone to
713 the accumulation of hybrid incompatibilities. In general, earlier developmental stages are

714 thought to be under greater pleiotropic constraint and less prone to disruption (Cutter and
715 Bundus 2020). With the progression of mouse spermatogenesis, pleiotropy decreases (as
716 approximated by increases in tissue specificity; Murat *et al.* 2023) and the rate of protein-
717 coding evolution increases (Larson *et al.* 2016; Kopania *et al.* 2022a; Murat *et al.* 2023), which
718 may make the later stages of spermatogenesis more prone to accumulating hybrid
719 incompatibilities. Indeed, we found fewer DE genes both between parent species and in sterile
720 hybrids for both dwarf hamsters and house mice during the early stages of spermatogenesis
721 than in later stages (Figures S9 and S10), and hybrid misexpression greatly exceeds parental
722 expression divergence in late spermatogenesis. Despite general similarity in patterns of
723 misexpression across spermatogenesis in hybrids, we found that few DE genes were shared
724 between dwarf hamster and house mouse hybrids, suggesting that shared genes of large
725 effect are unlikely to be responsible for the repeated evolution of hybrid male sterility. The low
726 levels of disrupted gene expression early in spermatogenesis that we and others have shown
727 suggests that there might be some tolerance for misregulation early in spermatogenesis, since
728 misregulation of some genes during early stages does not always completely halt the
729 progression of sperm development (Oka *et al.* 2010; Ishishita *et al.* 2015; Mipam *et al.* 2023).
730 However, the patterns we find in dwarf hamsters suggests that spermatogenesis may be
731 disrupted between zygotene and diplotene cell stages from early misexpression. Dwarf
732 hamster hybrid diplotene cell populations had X-linked and autosomal gene expression profiles
733 which more closely resemble parental leptotene/zygotene cell populations than either diplotene
734 or postmeiotic cell populations. Furthermore, DE genes in hybrids during diplotene were
735 enriched for genes associated with cell differentiation, proliferation, and programmed cell
736 death, suggesting misexpression during this stage could be a consequence of a stalling or
737 breakdown of early meiosis in hybrid dwarf hamsters. It's unclear what underlying genomic
738 mechanisms could result in this breakdown, but it is possible that this disruption could

739 potentially act as a major contributor to hybrid sterility in this system. Ultimately, we find that
740 spermatogenesis is a complex and rapidly evolving developmental program that may provide
741 many potential avenues across its timeline for the evolution of hybrid incompatibilities.
742

743 **Abnormal sex chromosome expression in dwarf hamster hybrids is inconsistent with**
744 **disrupted MSCI**

745 The sex chromosomes play a central role in speciation, an observation which has been
746 supported by both Haldane's rule (Haldane 1922) and the large X-effect on hybrid male sterility
747 (Coyne and Orr 1989). Misregulation of the X chromosome may contribute to hybrid sterility in
748 several species pairs (Davis *et al.* 2015; Morgan *et al.* 2020; Sánchez-Ramírez *et al.* 2021). The
749 X chromosome is transcriptionally repressed during routine spermatogenesis in many
750 organisms including eutherian mammals (McKee and Handel 1993), monotremes (Murat *et al.*
751 2023), *Drosophila* (Landeen *et al.* 2016), grasshoppers (Viera *et al.* 2021), mosquitos (Taxiarchi
752 *et al.* 2019), and nematodes (Rappaport *et al.* 2021). Because of the ubiquity of X chromosome
753 repression during spermatogenesis, disruption of transcriptional repression could be a
754 widespread regulatory phenotype in sterile hybrids (Lifschytz and Lindsley 1972; Larson *et al.*
755 2018). In sterile hybrid mice, disrupted X repression (disrupted MSCI) leads to the
756 overexpression of the normally silenced X chromosome during diplotene (Good *et al.* 2010;
757 Bhattacharyya *et al.* 2013; Campbell *et al.* 2013; Turner and Harr 2014; Larson *et al.* 2017,
758 2022). We also found overexpression of the X chromosome during diplotene in sterile hybrid
759 dwarf hamsters, but in a manner inconsistent with disrupted MSCI. Both the X chromosome
760 and autosomes are overexpressed in dwarf hamster hybrid diplotene cells to a greater extent
761 on average than was observed in house mice, and importantly, X-linked overexpression was
762 more variable in dwarf hamster hybrids than house mice hybrids. In fact, some dwarf hamster
763 hybrids had wildly overexpressed X chromosomes while others appeared to have properly

764 silenced X chromosomes. Our expression correlation and gene set analyses of hybrid diplotene
765 cells provide additional evidence that the genes overexpressed in hybrid hamster diplotene are
766 different than those overexpressed in house mouse hybrids, sharing more similarity to the
767 earlier meiotic cell types than downstream postmeiotic cell types. Overall, our results indicate
768 fundamentally different patterns of X-linked overexpression in both systems, with X-linked
769 overexpression in dwarf hamster hybrids being inconsistent with disrupted MSCI.

770 Much of what we know about the genomic architecture and the role of sex
771 chromosome misregulation in hybrid male sterility in mammals comes from decades of work
772 that have shown a major gene, *Prdm9*, and its X chromosome modulator, *Hstx2*, may be
773 responsible for most F1 hybrid male sterility in house mice (Forejt *et al.* 1991, 2021; Trachtulec
774 *et al.* 1997; Mihola *et al.* 2009; Lustyk *et al.* 2019). *Prdm9* directs the location of double strand
775 breaks during meiotic recombination (Mihola *et al.* 2009; Oliver *et al.* 2009; Smagulova *et al.*
776 2016). In hybrid mice, divergence at *Prdm9* binding sites leads to asymmetric double-stranded
777 breaks and results in autosomal asynapsis, triggering Meiotic Silencing of Unsynapsed
778 Chromatin, shutting down transcription on asynapsed autosomes using the same cellular
779 machinery as MSCI (Turner 2015), and eventually meiotic arrest and cell death (Bhattacharyya
780 *et al.* 2013; Forejt *et al.* 2021). This process is associated with the disruption of MSCI and a
781 characteristic overexpression of the X chromosome during meiosis (Good *et al.* 2010;
782 Bhattacharyya *et al.* 2013; Campbell *et al.* 2013; Turner and Harr 2014; Larson *et al.* 2017,
783 2022), but whether disrupted MSCI directly contributes to hybrid male sterility or is simply a
784 downstream consequence of *Prdm9* divergence is still uncertain (Forejt *et al.* 2021).

785 Whether we should have expected patterns of disrupted sex chromosome expression
786 in sterile hybrid hamsters to be the same as house mice is unclear. The sex chromosomes in
787 pachytene cells of hybrid dwarf hamsters display normal yH2AFX staining (Ishishita *et al.* 2015;
788 Bikchurina *et al.* 2018), a key marker in MSCI (Abe *et al.* 2022), which may indicate that the

789 hybrid sex chromosomes are properly silenced. Additionally, autosomal asynapsis is rarely
790 observed in hybrid dwarf hamsters, and asynapsis is almost exclusive to the sex chromosomes
791 (Ishishita *et al.* 2015; Bikchurina *et al.* 2018). This contrasts *Prdm9*-mediated sterility in house
792 mice, where hybrid autosomes are often asynapsed and decorated with yH2AFX
793 (Bhattacharyya *et al.* 2013; Forejt *et al.* 2021). Mechanisms other than *Prdm9* may also disrupt
794 MSCI and result in sterility, such as macrosatellite copy number divergence (Bredemeyer *et al.*
795 2021) and X-autosome translocations that impair synapsis (Homolka *et al.* 2007), although
796 there is no evidence for X-autosome translocations between these two species of dwarf
797 hamsters (Moore *et al.* 2022). Thus, while MSCI may be a major target for the accumulation of
798 reproductive barriers between species in many mammalian systems, either through *Prdm9*
799 divergence or alternative mechanisms, our results suggest that sterility in dwarf hamsters has a
800 more composite regulatory basis.

801 Another mechanism often proposed to underlie mammalian male hybrid sterility,
802 especially in rodents, is divergence in the PAR between parental species. The PAR is the only
803 portion of the sex chromosomes which can synapse during spermatogenesis, and it is still
804 unclear if the regulation of the PAR is uniformly detached from MSCI across divergent
805 mammalian sex chromosome systems (Raudsepp and Chowdhary 2015). We find no evidence
806 that PAR-specific misregulation is associated with hybrid sterility in dwarf hamsters. PAR
807 genes are not silenced in hybrids or parents, a pattern that is inconsistent with MSCI that has
808 extended to the PAR due to XY asynapsis, and further, expression of PAR genes in hybrids
809 differs little from parental PAR expression. While we find no evidence that PAR misregulation
810 *per se* is associated with hybrid sterility in this system, we cannot rule out the possibility that
811 structural and sequence divergence between the PARs of *P. sungorus* and *P. campbelli* may
812 be associated with hybrid sterility. Structural and sequence divergence in the PAR has been
813 hypothesized to activate the meiotic spindle checkpoint by interfering with proper pairing of

sex chromosomes (Burgoyne *et al.* 2009; Dumont 2017). The PAR evolves rapidly in rodents (White *et al.* 2012b; Raudsepp and Chowdhary 2015; Morgan *et al.* 2019), and this elevated divergence may underlie sex chromosome asynapsis and apoptosis in several hybrid mouse crosses (Matsuda *et al.* 1991; Oka *et al.* 2010; White *et al.* 2012a; Dumont 2017). Furthermore, divergence in the mouse PAR has been implicated in spermatogenic defects in crosses where *Prdm9*-divergence is minimal, such as between closely related subspecies (Dumont 2017) or in mice with genetically-modified *Prdm9* alleles (Davies *et al.* 2021). Meiosis is likely tolerant to some degree of divergence in the PAR (Morgan *et al.* 2019), but exact limits are currently unknown. At this time, thorough analysis of structural and sequence divergence between the PARs in dwarf hamsters is challenging as the PAR is notoriously difficult to assemble (but see Kasahara *et al.* 2022), and there are annotation gaps in the current assembly of the PAR in dwarf hamsters. In sum, we find no clear pattern of regulatory disruption of PAR genes in sterile hybrid dwarf hamsters, though this result may change pending further refinement of the PAR annotation.

Conclusions

Cell-specific approaches for quantifying expression phenotypes are powerful tools for providing insight into the underlying mechanisms behind hybrid dysfunction (Hunnicutt *et al.* 2022), especially in systems where it remains difficult to interrogate the underlying genomic architecture of these traits. Using a contrast of dwarf hamster and house mouse hybrids, we have shown that transgressive overexpression is not an inevitable outcome of hybridization, that hybrid incompatibilities are likely to arise during multiple stages of spermatogenesis, and that disrupted sex chromosome silencing does not appear to play an equal role in sterility between these two systems. Both the expression phenotypes we observed here and histological evidence from other studies (Ishishita *et al.* 2015; Bikchurina *et al.* 2018) suggest

that several reproductive barriers are acting during spermatogenesis in dwarf hamster hybrids. It has become increasingly apparent as more study systems are investigated that the genetic basis of postzygotic species barriers are often complex and polymorphic (Cutter 2012; Coughlan and Matute 2020), and implementing approaches which account for the developmental complexities of hybrid dysfunction, as we have done here, will allow us to make further advances in understanding the processes of speciation.

Acknowledgements:

This work was supported by a National Science Foundation Graduate Research Fellowship to KEH (DGE-2034612) and the following grants awarded to KEH: Sigma Xi Grant-in-aid of Research, American Society of Mammalogists Grant-in-Aid of Research Grant, and a Society for the Study of Evolution R.C. Lewontin Early Award. Additionally, this work was supported by grants from the Eunice Kennedy Shriver National Institute of Child Health and Human Development of the National Institutes of Health (R01-HD073439, R01-HD094787) to JMG, and the National Science Foundation to ELL (DEB-2012041). We would like to thank members of the Larson and Good labs, as well as Jonathan Velotta and members of the Velotta lab, for feedback on this project, Gabrielle Welsh for technical assistance, Ivan Kovanda for support using the University of Denver Research Data Analysis Cluster, and Pamela K. Shaw and the UM Fluorescence Cytometry Core supported by an Institutional Development Award from the NIGMS (P30GM103338). Any opinions, findings, and conclusions or recommendations expressed in this material are those of the author(s) and do not necessarily reflect the views of the National Science Foundation or the National Institutes of Health.

Author contributions:

KEH, JMG, and ELL conceived of the study. CC, SK, ELL, and KEH conducted lab work. KEH conducted the analyses. KEH and ELL wrote the manuscript with input from ECM, CC, SK, and JMG.

Data accessibility:

Hamster sequence data are available through the NCBI SRA under accession number PRJNA1024468, and mouse sequence data are available under SRA accession PRJNA296926. File S1 contains all supplemental figures. Code used for the analyses and fertility phenotypic data are available from GitHub (https://github.com/KelsieHunnicutt/dwarf_hamster_hybrids).

870 **LITERATURE CITED**
871

872 Abe H., Y.-H. Yeh, Y. Munakata, K.-I. Ishiguro, P. R. Andreassen, *et al.*, 2022 Active DNA
873 damage response signaling initiates and maintains meiotic sex chromosome
874 inactivation. Nat. Commun. 13: 7212.

875 Anders S., and W. Huber, 2010 Differential expression analysis for sequence count data.
876 Nature Precedings 1–1.

877 Barreto F. S., R. J. Pereira, and R. S. Burton, 2015 Hybrid dysfunction and physiological
878 compensation in gene expression. Mol. Biol. Evol. 32: 613–622.

879 Bayes J. J., and H. S. Malik, 2009 Altered heterochromatin binding by a hybrid sterility protein
880 in Drosophila sibling species. Science 326: 1538–1541.

881 Benjamini Y., and Y. Hochberg, 1995 Controlling the false discovery rate: a practical and
882 powerful approach to multiple testing. J. R. Stat. Soc. 57: 289–300.

883 Bhattacharyya T., S. Gregorova, O. Mihola, M. Anger, J. Sebestova, *et al.*, 2013 Mechanistic
884 basis of infertility of mouse intersubspecific hybrids. Proc. Natl. Acad. Sci. U. S. A. 110:
885 E468–E477.

886 Bikchurina T. I., K. V. Tishakova, E. A. Kizilova, S. A. Romanenko, N. A. Serdyukova, *et al.*,
887 2018 Chromosome synapsis and recombination in male-sterile and female-fertile
888 interspecies hybrids of the dwarf hamsters (Phodopus, Cricetidae). Genes 9: 227.

889 Bolger A. M., M. Lohse, and B. Usadel, 2014 Trimmomatic: a flexible trimmer for Illumina
890 sequence data. Bioinformatics 30: 2114–2120.

891 Bredemeyer K. R., C. M. Seabury, M. J. Stickney, J. R. McCarrey, B. M. vonHoldt, *et al.*, 2021

892 Rapid macrosatellite evolution promotes X-linked hybrid male sterility in a feline
893 interspecies cross. Mol. Biol. Evol. 38: 5588–5609.

894 Brekke T. D., and J. M. Good, 2014 Parent-of-origin growth effects and the evolution of hybrid
895 inviability in dwarf hamsters. Evolution 68: 3134–3148.

896 Brekke T. D., L. A. Henry, and J. M. Good, 2016 Genomic imprinting, disrupted placental
897 expression, and speciation. Evolution 70: 2690–2703.

898 Brekke T. D., K. A. Steele, and J. F. Mulley, 2018 Inbred or outbred? Genetic diversity in
899 laboratory rodent colonies. G3 8: 679–686.

900 Brekke T. D., E. C. Moore, S. C. Campbell-Staton, C. M. Callahan, Z. A. Cheviron, *et al.*, 2021 X
901 chromosome-dependent disruption of placental regulatory networks in hybrid dwarf
902 hamsters. Genetics 218: iyab043.

903 Burgoyne P. S., 1982 Genetic homology and crossing over in the X and Y chromosomes of
904 mammals. Hum. Genet. 61: 85–90.

905 Burgoyne P. S., S. K. Mahadevaiah, and J. M. A. Turner, 2009 The consequences of asynapsis
906 for mammalian meiosis. Nat. Rev. Genet. 10: 207–216.

907 Campbell P., J. M. Good, and M. W. Nachman, 2013 Meiotic sex chromosome inactivation is
908 disrupted in sterile hybrid male house mice. Genetics 193: 819–828.

909 Civetta A., 2016 Misregulation of gene expression and sterility in interspecies hybrids: causal
910 links and alternative hypotheses. J. Mol. Evol. 82: 176–182.

911 Coughlan J. M., and D. R. Matute, 2020 The importance of intrinsic postzygotic barriers
912 throughout the speciation process. Philos. Trans. R. Soc. Lond. B Biol. Sci. 375:

913 20190533.

914 Coyne J. A., and H. A. Orr, 1989 Two rules of speciation, pp. 180–207 in *Speciation and its*
915 *consequences*, edited by Otte D., Endler J. A. Sinauer Associates, Sunderland, MA.

916 Cutter A. D., 2012 The polymorphic prelude to Bateson-Dobzhansky-Muller incompatibilities.
917 Trends Ecol. Evol. 27: 209–218.

918 Cutter A. D., and J. D. Bundus, 2020 Speciation and the developmental alarm clock. Elife 9:
919 e56276.

920 Danecek P., A. Auton, G. Abecasis, C. A. Albers, E. Banks, *et al.*, 2011 The variant call format
921 and VCFtools. Bioinformatics 27: 2156–2158.

922 Davies B., E. Hatton, N. Altemose, J. G. Hussin, F. Pratto, *et al.*, 2016 Re-engineering the zinc
923 fingers of PRDM9 reverses hybrid sterility in mice. Nature 530: 171–176.

924 Davies B., A. Gupta Hinch, A. Cebrian-Serrano, S. Alghadban, P. W. Becker, *et al.*, 2021
925 Altering the binding properties of PRDM9 partially restores fertility across the species
926 boundary. Mol. Biol. Evol. 38: 5555–5562.

927 Davis B. W., C. M. Seabury, W. A. Brashear, G. Li, M. Roelke-Parker, *et al.*, 2015 Mechanisms
928 underlying mammalian hybrid sterility in two feline interspecies models. Mol. Biol. Evol.
929 32: 2534–2546.

930 Dumont B. L., 2017 Meiotic consequences of genetic divergence across the murine
931 pseudoautosomal region. Genetics 205: 1089–1100.

932 Ellis N., and P. N. Goodfellow, 1989 The mammalian pseudoautosomal region. Trends Genet.
933 5: 406–410.

934 Forejt J., V. Vincek, J. Klein, H. Lehrach, and M. Loudová-Micková, 1991 Genetic mapping of
935 the t-complex region on mouse chromosome 17 including the Hybrid sterility-1 gene.
936 Mamm. Genome 1: 84–91.

937 Forejt J., P. Jansa, and E. Parvanov, 2021 Hybrid sterility genes in mice (Mus musculus): a
938 peculiar case of PRDM9 incompatibility. Trends Genet. 37: 1095–1108.

939 Gamperl R., G. Vistorin, and W. Rosenkranz, 1977 New observations on the karyotype of the
940 Djungarian hamster, Phodopus sungorus. Experientia 33: 1020–1021.

941 Getun I. V., B. Torres, and P. R. J. Bois, 2011 Flow cytometry purification of mouse meiotic
942 cells. J. Vis. Exp. e2602.

943 Good J. M., M. A. Handel, and M. W. Nachman, 2008 Asymmetry and polymorphism of hybrid
944 male sterility during the early stages of speciation in house mice. Evolution 62: 50–65.

945 Good J. M., T. Giger, M. D. Dean, and M. W. Nachman, 2010 Widespread over-expression of
946 the X chromosome in sterile F1 hybrid mice. PLoS Genet. 6: e1001148.

947 Green C. D., Q. Ma, G. L. Manske, A. N. Shami, X. Zheng, *et al.*, 2018 A comprehensive
948 roadmap of murine spermatogenesis defined by single-cell RNA-Seq. Dev. Cell 46:
949 651-667.e10.

950 Gu Z., R. Eils, and M. Schlesner, 2016 Complex heatmaps reveal patterns and correlations in
951 multidimensional genomic data. Bioinformatics 32: 2847–2849.

952 Guerrero R. F., A. L. Posto, L. C. Moyle, and M. W. Hahn, 2016 Genome-wide patterns of
953 regulatory divergence revealed by introgression lines. Evolution 70: 696–706.

954 Haaf T., H. Weis, and M. Schmid, 1987 A comparative cytogenetic study on the mitotic and

955 meiotic chromosomes in hamster species of the genus Phodopus (Rodentia,
956 Cricetinae). Zeitschrift für Säugetierkunde 52: 281–290.

957 Haerty W., and R. S. Singh, 2006 Gene regulation divergence is a major contributor to the
958 evolution of Dobzhansky-Muller incompatibilities between species of Drosophila. Mol.
959 Biol. Evol. 23: 1707–1714.

960 Haldane J. B. S., 1922 Sex ratio and unisexual sterility in hybrid animals. J. Genet. 12: 101–
961 109.

962 Handel M. A., 2004 The XY body: a specialized meiotic chromatin domain. Exp. Cell Res. 296:
963 57–63.

964 Hermann B. P., K. Cheng, A. Singh, L. Roa-De La Cruz, K. N. Mutoji, *et al.*, 2018 The
965 mammalian spermatogenesis single-cell transcriptome, from spermatogonial stem cells
966 to spermatids. Cell Rep. 25: 1650-1667.e8.

967 Holt J., S. Huang, L. McMillan, and W. Wang, 2013 Read annotation pipeline for high-
968 throughput sequencing data, pp. 605–612 in *Proceedings of the International*
969 *Conference on Bioinformatics, Computational Biology and Biomedical Informatics -*
970 *BCB'13*, ACM Press, New York, New York, USA.

971 Homolka D., R. Ivanek, J. Capkova, P. Jansa, and J. Forejt, 2007 Chromosomal rearrangement
972 interferes with meiotic X chromosome inactivation. Genome Res. 17: 1431–1437.

973 Huang S., J. Holt, C.-Y. Kao, L. McMillan, and W. Wang, 2014 A novel multi-alignment pipeline
974 for high-throughput sequencing data. Database 2014: bau057.

975 Hunnicutt K. E., J. M. Good, and E. L. Larson, 2022 Unraveling patterns of disrupted gene

expression across a complex tissue. Evolution 76: 275–291.

Ishishita S., K. Tsuboi, N. Ohishi, K. Tsuchiya, and Y. Matsuda, 2015 Abnormal pairing of X and Y sex chromosomes during meiosis I in interspecific hybrids of Phodopus campbelli and P. sungorus. Sci. Rep. 5: 9435.

Kasahara T., K. Mekada, K. Abe, A. Ashworth, and T. Kato, 2022 Complete sequencing of the mouse pseudoautosomal region, the most rapidly evolving 'chromosome.' bioRxiv 2022.03.26.485930.

Kim D., J. M. Paggi, C. Park, C. Bennett, and S. L. Salzberg, 2019 Graph-based genome alignment and genotyping with HISAT2 and HISAT-genotype. Nat. Biotechnol. 37: 907–915.

Kolberg L., U. Raudvere, I. Kuzmin, J. Vilo, and H. Peterson, 2020 gprofiler2 -- an R package for gene list functional enrichment analysis and namespace conversion toolset g:Profiler. F1000Res. 9. https://doi.org/10.12688/f1000research.24956.2

Kopania E. E. K., E. L. Larson, C. Callahan, S. Keeble, and J. M. Good, 2022a Molecular evolution across mouse spermatogenesis. Mol. Biol. Evol. 39: msac023.

Kopania E. E. K., E. M. Watson, C. C. Rathje, B. M. Skinner, P. J. I. Ellis, *et al.*, 2022b The contribution of sex chromosome conflict to disrupted spermatogenesis in hybrid house mice. Genetics 222: iyac151.

Korunes K. L., and K. Samuk, 2021 pixy: Unbiased estimation of nucleotide diversity and divergence in the presence of missing data. Mol. Ecol. Resour. 21: 1359–1368.

Kousathanas A., D. L. Halligan, and P. D. Keightley, 2014 Faster-X adaptive protein evolution in

house mice. Genetics 196: 1131–1143.

Lafon-Placette C., and C. Köhler, 2015 Epigenetic mechanisms of postzygotic reproductive isolation in plants. Curr. Opin. Plant Biol. 23: 39–44.

Landeen E. L., C. A. Muirhead, L. Wright, C. D. Meiklejohn, and D. C. Presgraves, 2016 Sex chromosome-wide transcriptional suppression and compensatory cis-regulatory evolution mediate gene expression in the Drosophila male germline. PLoS Biol. 14: e1002499.

Larson E. L., D. Vanderpool, S. Keeble, M. Zhou, B. A. J. Sarver, *et al.*, 2016 Contrasting levels of molecular evolution on the mouse X chromosome. Genetics 203: 1841–1857.

Larson E. L., S. Keeble, D. Vanderpool, M. D. Dean, and J. M. Good, 2017 The composite regulatory basis of the large X-effect in mouse speciation. Mol. Biol. Evol. 34: 282–295.

Larson E. L., E. E. K. Kopania, and J. M. Good, 2018 Spermatogenesis and the evolution of mammalian sex chromosomes. Trends Genet. 34: 722–732.

Larson E. L., E. E. K. Kopania, K. E. Hunnicutt, D. Vanderpool, S. Keeble, *et al.*, 2022 Stage-specific disruption of X chromosome expression during spermatogenesis in sterile house mouse hybrids. G3 12: jkab407.

Liao Y., G. K. Smyth, and W. Shi, 2014 featureCounts: an efficient general purpose program for assigning sequence reads to genomic features. Bioinformatics 30: 923–930.

Lifschytz E., and D. L. Lindsley, 1972 The role of X-chromosome inactivation during spermatogenesis. Proc. Natl. Acad. Sci. U. S. A. 69: 182–186.

Llopart A., 2012 The rapid evolution of X-linked male-biased gene expression and the large-X

1018 effect in Drosophila yakuba, D. santomea, and their hybrids. Mol. Biol. Evol. 29: 3873–
1019 3886.

1020 Luo H., T. Mipam, S. Wu, C. Xu, C. Yi, *et al.*, 2022 DNA methylome of primary spermatocyte
1021 reveals epigenetic dysregulation associated with male sterility of cattleyak.
1022 Theriogenology 191: 153–167.

1023 Lustyk D., S. Kinský, K. K. Ullrich, M. Yancoskie, L. Kašíková, *et al.*, 2019 Genomic structure of
1024 Hstx2 modifier of Prdm9-dependent hybrid male sterility in mice. Genetics 213: 1047–
1025 1063.

1026 Mack K. L., P. Campbell, and M. W. Nachman, 2016 Gene regulation and speciation in house
1027 mice. Genome Res. 26: 451–461.

1028 Mack K. L., and M. W. Nachman, 2017 Gene regulation and speciation. Trends Genet. 33: 68–
1029 80.

1030 Matsuda Y., T. Hirobe, and V. M. Chapman, 1991 Genetic basis of X-Y chromosome
1031 dissociation and male sterility in interspecific hybrids. Proc. Natl. Acad. Sci. U. S. A. 88:
1032 4850–4854.

1033 McCarthy D. J., Y. Chen, and G. K. Smyth, 2012 Differential expression analysis of multifactor
1034 RNA-Seq experiments with respect to biological variation. Nucleic Acids Res. 40: 4288–
1035 4297.

1036 McKee B. D., and M. A. Handel, 1993 Sex chromosomes, recombination, and chromatin
1037 conformation. Chromosoma 102: 71–80.

1038 McManus C. J., J. D. Coolon, M. O. Duff, J. Eipper-Mains, B. R. Graveley, *et al.*, 2010

1039 Regulatory divergence in Drosophila revealed by mRNA-seq. Genome Res. 20: 816–
1040 825.

1041 Meiklejohn C. D., J. D. Coolon, D. L. Hartl, and P. J. Wittkopp, 2014 The roles of cis- and trans-
1042 regulation in the evolution of regulatory incompatibilities and sexually dimorphic gene
1043 expression. Genome Res. 24: 84–95.

1044 Michalak P., and M. A. F. Noor, 2003 Genome-wide patterns of expression in Drosophila pure
1045 species and hybrid males. Mol. Biol. Evol. 20: 1070–1076.

1046 Mihola O., Z. Trachtulec, C. Vlcek, J. C. Schimenti, and J. Forejt, 2009 A mouse speciation
1047 gene encodes a meiotic histone H3 methyltransferase. Science 323: 373–375.

1048 Mipam T., X. Chen, W. Zhao, P. Zhang, Z. Chai, *et al.*, 2023 Single-cell transcriptome analysis
1049 and in vitro differentiation of testicular cells reveal novel insights into male sterility of the
1050 interspecific hybrid cattle-yak. BMC Genomics 24: 149.

1051 Montgomery S. H., and J. E. Mank, 2016 Inferring regulatory change from gene expression: the
1052 confounding effects of tissue scaling. Mol. Ecol. 25: 5114–5128.

1053 Moore E. C., G. W. C. Thomas, S. Mortimer, E. E. K. Kopania, K. E. Hunnicutt, *et al.*, 2022 The
1054 evolution of widespread recombination suppression on the dwarf hamster (Phodopus) X
1055 chromosome. Genome Biol. Evol. 14: evac080.

1056 Morgan A. P., T. A. Bell, J. J. Crowley, and F. Pardo-Manuel de Villena, 2019 Instability of the
1057 pseudoautosomal boundary in house mice. Genetics 212: 469–487.

1058 Morgan K., B. Harr, M. A. White, B. A. Payseur, and L. M. Turner, 2020 Disrupted gene
1059 networks in subfertile hybrid house mice. Mol. Biol. Evol. 37: 1547–1562.

1060 Mugal C. F., M. Wang, N. Backström, D. Wheatcroft, M. Ålund, *et al.*, 2020 Tissue-specific
1061 patterns of regulatory changes underlying gene expression differences among *Ficedula*
1062 flycatchers and their naturally occurring F1 hybrids. Genome Res. 30: 1727–1739.

1063 Murat F., N. Mbengue, S. B. Winge, T. Trefzer, E. Leushkin, *et al.*, 2023 The molecular evolution
1064 of spermatogenesis across mammals. Nature 613: 308–316.

1065 Namekawa S. H., P. J. Park, L.-F. Zhang, J. E. Shima, J. R. McCarrey, *et al.*, 2006 Postmeiotic
1066 sex chromatin in the male germline of mice. Curr. Biol. 16: 660–667.

1067 Neumann K., J. Michaux, V. Lebedev, N. Yigit, E. Colak, *et al.*, 2006 Molecular phylogeny of the
1068 Cricetinae subfamily based on the mitochondrial cytochrome b and 12S rRNA genes
1069 and the nuclear vWF gene. Mol. Phylogenet. Evol. 39: 135–148.

1070 Ogle D., and M. D. Ogle, 2017 Package 'FSA.' CRAN Repos 1–206.

1071 Oka A., A. Mita, Y. Takada, H. Koseki, and T. Shiroishi, 2010 Reproductive isolation in hybrid
1072 mice due to spermatogenesis defects at three meiotic stages. Genetics 186: 339–351.

1073 Oka A., and T. Shiroishi, 2014 Regulatory divergence of X-linked genes and hybrid male
1074 sterility in mice. Genes Genet. Syst. 89: 99–108.

1075 Oka A., T. Takada, H. Fujisawa, and T. Shiroishi, 2014 Evolutionarily diverged regulation of X-
1076 chromosomal genes as a primal event in mouse reproductive isolation. PLoS Genet. 10:
1077 e1004301.

1078 Oksanen J., F. G. Blanchet, R. Kindt, P. Legendre, P. R. Minchin, *et al.*, 2013 Package 'vegan.'
1079 Community ecology package, version 2: 1–295.

1080 Oliver P. L., L. Goodstadt, J. J. Bayes, Z. Birtle, K. C. Roach, *et al.*, 2009 Accelerated evolution

1081 of the Prdm9 speciation gene across diverse metazoan taxa. PLoS Genet. 5: e1000753.

1082 Ortíz-Barrientos D., B. A. Counterman, and M. A. F. Noor, 2007 Gene expression divergence
1083 and the origin of hybrid dysfunctions. Genetica 129: 71–81.

1084 Paun O., M. F. Fay, D. E. Soltis, and M. W. Chase, 2007 Genetic and epigenetic alterations
1085 after hybridization and genome doubling. Taxon 56: 649–656.

1086 Presgraves D. C., 2008 Sex chromosomes and speciation in Drosophila. Trends Genet. 24:
1087 336–343.

1088 Ramm S. A., and L. Schärer, 2014 The evolutionary ecology of testicular function: size isn't
1089 everything. Biol. Rev. Camb. Philos. Soc. 89: 874–888.

1090 Rappaport Y., H. Achache, R. Falk, O. Murik, O. Ram, *et al.*, 2021 Bisection of the X
1091 chromosome disrupts the initiation of chromosome silencing during meiosis in
1092 Caenorhabditis elegans. Nat. Commun. 12: 4802.

1093 Raudsepp T., and B. P. Chowdhary, 2015 The eutherian pseudoautosomal region. Cytogenet.
1094 Genome Res. 147: 81–94.

1095 Raymond C. S., M. W. Murphy, M. G. O'Sullivan, V. J. Bardwell, and D. Zarkower, 2000 Dmrt1,
1096 a gene related to worm and fly sexual regulators, is required for mammalian testis
1097 differentiation. Genes Dev. 14: 2587–2595.

1098 Ritchie M. E., B. Phipson, D. Wu, Y. Hu, C. W. Law, *et al.*, 2015 limma powers differential
1099 expression analyses for RNA-sequencing and microarray studies. Nucleic Acids Res.
1100 43: e47.

1101 Robinson M. D., D. J. McCarthy, and G. K. Smyth, 2010 edgeR: a Bioconductor package for

1102 differential expression analysis of digital gene expression data. Bioinformatics 26: 139–
1103 140.

1104 Sánchez-Ramírez S., J. G. Weiss, C. G. Thomas, and A. D. Cutter, 2021 Widespread
1105 misregulation of inter-species hybrid transcriptomes due to sex-specific and sex-
1106 chromosome regulatory evolution. PLoS Genet. 17: e1009409.

1107 Scribner S. J., and K. E. Wynne-Edwards, 1994 Disruption of body temperature and behavior
1108 rhythms during reproduction in dwarf hamsters (Phodopus). Physiol. Behav. 55: 361–
1109 369.

1110 Shivaprasad P. V., R. M. Dunn, B. A. Santos, A. Bassett, and D. C. Baulcombe, 2012
1111 Extraordinary transgressive phenotypes of hybrid tomato are influenced by epigenetics
1112 and small silencing RNAs. EMBO J. 31: 257–266.

1113 Smagulova F., K. Brick, Y. Pu, R. D. Camerini-Otero, and G. V. Petukhova, 2016 The
1114 evolutionary turnover of recombination hot spots contributes to speciation in mice.
1115 Genes Dev. 30: 266–280.

1116 Swanson M. T., C. H. Oliveros, and J. A. Esselstyn, 2019 A phylogenomic rodent tree reveals
1117 the repeated evolution of masseter architectures. Proc. Biol. Sci. 286: 20190672.

1118 Taxiarchi C., N. Kranjc, A. Kriezis, K. Kyrou, F. Bernardini, *et al.*, 2019 High-resolution
1119 transcriptional profiling of Anopheles gambiae spermatogenesis reveals mechanisms of
1120 sex chromosome regulation. Sci. Rep. 9: 14841.

1121 Trachtulec Z., M. Mnuková-Fajdelová, R. M. Hamvas, S. Gregorová, W. E. Mayer, *et al.*, 1997
1122 Isolation of candidate hybrid sterility 1 genes by cDNA selection in a 1.1 megabase pair
1123 region on mouse chromosome 17. Mamm. Genome 8: 312–316.

1124 Turner L. M., M. A. White, D. Tautz, and B. A. Payseur, 2014 Genomic networks of hybrid
1125 sterility. PLoS Genet. 10: e1004162.

1126 Turner L. M., and B. Harr, 2014 Genome-wide mapping in a house mouse hybrid zone reveals
1127 hybrid sterility loci and Dobzhansky-Muller interactions. Elife 3: e02504.

1128 Turner J. M. A., 2015 Meiotic silencing in mammals. Annu. Rev. Genet. 49: 395–412.

1129 Vasimuddin M., S. Misra, H. Li, and S. Aluru, 2019 Efficient architecture-aware acceleration of
1130 BWA-MEM for multicore systems, pp. 314–324 in *2019 IEEE International Parallel and*
1131 *Distributed Processing Symposium (IPDPS)*, IEEE.

1132 Viera A., M. T. Parra, S. Arévalo, C. García de la Vega, J. L. Santos, *et al.*, 2021 X chromosome
1133 inactivation during grasshopper spermatogenesis. Genes 12: 1844.

1134 White M. A., M. Stubbings, B. L. Dumont, and B. A. Payseur, 2012a Genetics and evolution of
1135 hybrid male sterility in house mice. Genetics 191: 917–934.

1136 White M. A., A. Ikeda, and B. A. Payseur, 2012b A pronounced evolutionary shift of the
1137 pseudoautosomal region boundary in house mice. Mamm. Genome 23: 454–466.

1138 Wittkopp P. J., B. K. Haerum, and A. G. Clark, 2004 Evolutionary changes in cis and trans gene
1139 regulation. Nature 430: 85–88.

1140 Wu C. I., and A. W. Davis, 1993 Evolution of postmating reproductive isolation: the composite
1141 nature of Haldane's rule and its genetic bases. Am. Nat. 142: 187–212.

1142 Zhu W., B. Hu, C. Becker, E. S. Doğan, K. W. Berendzen, *et al.*, 2017 Altered chromatin
1143 compaction and histone methylation drive non-additive gene expression in an
1144 interspecific Arabidopsis hybrid. Genome Biol. 18: 157.